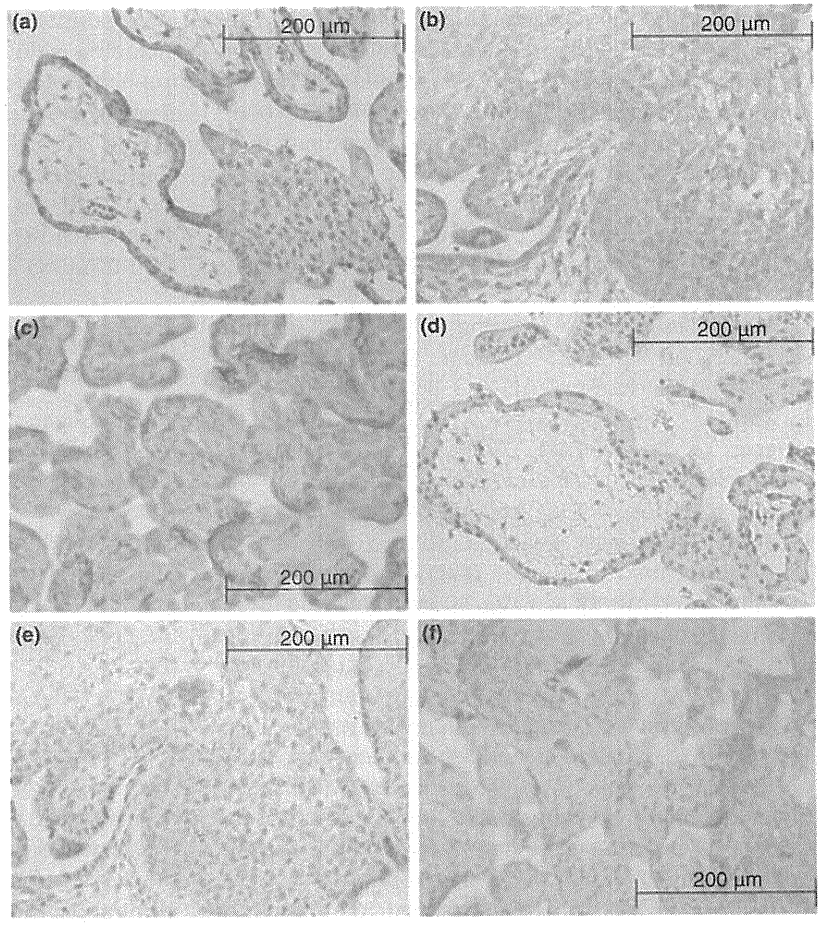

Fig. 1 The local distribution of autotaxin (ATX) protein in the first, second, and third trimester placenta. Immunohistochemical study was conducted to see the distributions of ATX protein in placentas at the first (a, d), second (b, e), and third (c, f) trimester using specific mAb to ATX (2A12) (a–c). No staining was detected in negative controls using isotype matched mouse IgG (d–f). Scale bar = 200 μm. The pictures shown are representative of the cases in each trimester.

the inter-villous cavity and the reconstruction of vascular structure of the uterine wall. In other way, some of villous cytotrophoblasts fuse, differentiate into villous syncytiotrophoblasts, and play multiple functions, such as substance exchange and hormone secretion in placenta.

Soluble ATX, which is produced by shedding of ATX, is the most important molecule for the regulation of extracellular concentration of LPA.[7–12] LPA has multiple functions including cellular proliferation, cellular differentiation, angiogenesis, and immune regulation.[1–5] ATX expressed by trophoblasts should be converted to soluble ATX, and then may work as a regulator for trophoblast proliferation, trophoblast differentiation, vascular remodeling, and feto-maternal immune interaction in placenta through the function of LPA.

Lysophosphatidic acid may also regulate implantation. Of the specific receptors to LPA, deletion of LPA_3 in mice was reported to result in reduced litter size.[19] Interestingly, LPA_3 expression in uterus was strictly up-regulated during early pregnancy and then returned to the basal level through the end of pregnancy.[24] LPA regulates immune responses with a control on migration and activation of lymphocytes and dendritic cells.[5] In implantation, early embryo is thought to need local inflammation to penetrate and invade in decidual tissue. ATX might work in implantation by producing LPA that may induce inflammation through the activation of lymphocytes and dendritic cells.

The activity of ATX was the highest at the third trimester of pregnancy and to a higher extent in patients in threatened pre-term delivery.[9] As for the receptors for LPA, LPA_1, mRNA level was identified in cultured myometrial cells from pregnant women; and in rat uterine LPA_1, mRNA level was elevated at the end of gestation.[25] Intravenous injection of LPA

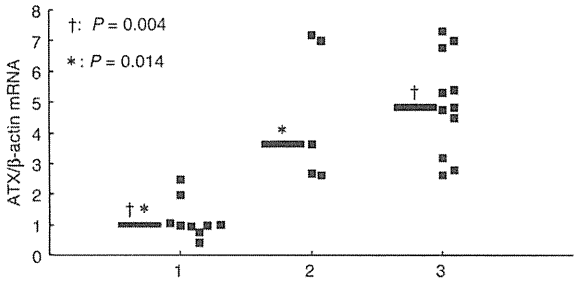

Fig. 2 The mRNA expression of ATX in the first, second, and third trimester placentas. Real-time PCR was conducted to investigate the amounts of ATX mRNA in the first, second, and third placenta tissues. The amounts of ATX mRNA after compensation with beta-actin mRNA amounts in the second trimester placenta (Lane 2; $n = 5$, 18 weeks, median 3.7, 5-percentile 2.6, 95-percentile 7.2) and the third trimester placenta (Lane 3; $n = 11$, 37–40 weeks, median 4.8, 5-percentile 2.7, 95-percentile 7.2) were higher than those in the first trimester placenta (Lane 1; $n = 9$, 6–11 weeks, median 1.0, 5-percentile 0.6, 95-percentile 2.3) ($P = 0.014$ (second versus first); $P = 0.004$ (third versus first). Data are represented by dots and median values are expressed by horizontal bars.

induced an immediate rise in intrauterine pressure, like prostaglandin F2 alpha.[26] Oxytocin receptor gene expression in the myometrial cells in primary culture from women in late gestation was up-regulated by the addition of LPA.[27] These findings suggested the roles of ATX and its product, LPA, in induction of labor.

Autotaxin activity in plasma increases paralleled with gestational weeks. To clarify the mechanism how ATX activity in plasma increases paralleled with gestational weeks, we performed real-time PCR to quantify mRNA of ATX in placenta at the first, second, and third trimester. As ATX protein exists in blood, we did not quantify ATX protein by Western blotting in placenta tissues, which contain much amount of blood. The real-time PCR revealed that the mRNA amounts of ATX in placenta tissues paralleled with gestational weeks, i.e. the ATX level in plasma, suggesting that the increase in the ATX level during pregnancy[9,18] is due to the increase in the production of mRNA by each cell as well as due to the increase in size of placenta, mostly in the number of trophoblasts, which might cause the increase in total amount of ATX protein produced by placenta.

In summary, we identified the molecules of ATX in placenta tissue, especially in trophoblasts and found that mRNA production of ATX in placenta tissues paralleled with gestational weeks, i.e. the ATX level in plasma. These findings suggest that trophoblasts might produce ATX and its bioactive resultant substance, LPA, paralleled with gestational weeks. This is the first report that proves controlled expression of ATX in human placenta.

References

1 Fukushima N, Ishii I, Contos JJA, Weiner JA, Chu J: Lysophospholipid receptors. *Annu Rev Pharmacol Toxicol* 2001; 41:507–534.

2 Goetzl EJ, An S: Diversity of cellular receptors and functions for the lysophospholipid growth factors lysophosphatidic acid and sphingosine 1-phosphate. *FASEB J* 1998; 12:1589–1598.

3 Moolenaar WH: Bioactive lysophospholipids and their G protein-coupled receptors. *Exp Cell Res* 1999; 253:230–238.

4 Tokumura A: A family of phospholipid autacoids: occurrence, metabolism and bioactions. *Prog Lipid Res* 1995; 34:151–184.

5 Georas SN: Lysophosphatidic acid and autotaxin: emerging roles in innate and adaptive immunity. *Immunol Res* 2009; Jan 30. doi: 10.1007/s12026-009-8104-y [Epub ahead of print].

6 Mills GB, Moolenaar WH: The emerging role of lysophosphatidic acid in cancer. *Nat Rev Cancer* 2003; 3:582–591.

7 Aoki J, Taira A, Takanezawa Y, Kishi Y, Hama K, Kishimoto T, Mizuno K, Saku K, Taguchi R, Arai H: Serum lysophosphatidic acid is produced through diverse phospholipase pathways. *J Biol Chem* 2002; 277:48737–48744.

8 Umezu-Goto M, Kishi Y, Taira A, Hama K, Dohmae N, Takio K, Yamori T, Mills GB, Inoue K, Aoki J, Arai H: Autotaxin has lysophospholipase D activity leading to tumor cell growth and motility by lysophosphatidic acid production. *J Cell Biol* 2002; 158:227–233.

9 Tokumura A, Majima E, Kariya Y, Tominaga K, Kogure K, Yasuda K, Fukuzawa K: Identification of human plasma lysophospholipase D, a lysophosphatidic acid-producing enzyme, as autotaxin, a multifunctional phosphodiesterase. *J Biol Chem* 2002; 277:39436–39442.

10 Hosogaya S, Yatomi Y, Nakamura K, Ohkawa R, Okubo S, Yokota H, Ohta M, Yamazaki H, Koike T, Ozaki Y: Measurement of plasma lysophosphatidic acid concentration in healthy subjects: strong correlation with lysophospholipase D activity. *Ann Clin Biochem* 2008; 45:364–368.

11 Watanabe N, Ikeda H, Nakamura K, Ohkawa R, Kume Y, Aoki J, Hama K, Okudaira S, Tanaka M,

Tomiya T, Yanase M, Tejima K, Nishikawa T, Arai M, Arai H, Omata M, Fujiwara K, Yatomi Y: Both plasma lysophosphatidic acid and serum autotaxin levels are increased in chronic hepatitis C. *J Clin Gastroenterol* 2007; 41:616–623.

12 Masuda A, Nakamura K, Izutsu K, Igarashi K, Ohkawa R, Jona M, Higashi K, Yokota H, Okudaira S, Kishimoto T, Watanabe T, Koike Y, Ikeda H, Kozai Y, Kurokawa M, Aoki J, Yatomi Y: Serum autotaxin measurement in haematological malignancies: a promising marker for follicular lymphoma. *Br J Haematol* 2008; 143:60–70.

13 Tanaka M, Okudaira S, Kishi Y, Ohkawa R, Iseki S, Ota M, Noji S, Yatomi Y, Aoki J, Arai H: Autotaxin stabilizes blood vessels and is required for embryonic vasculature by producing lysophosphatidic acid. *J Biol Chem* 2006; 281:25822–25830.

14 Tokumura A, Miyake M, Nishioka Y, Yamano S, Aono T, Fukuzawa K: Production of lysophosphatidic acids by lysophospholipase D in human follicular fluids of In vitro fertilization patients. *Biol Reprod* 1999; 61:195–199.

15 Hinokio K, Yamano S, Nakagawa K, Irahara M, Kamada M, Tokumura A, Aono T: Lysophosphatidic acid stimulates nuclear and cytoplasmic maturation of golden hamster immature oocytes in vitro via cumulus cells. *Life Sci* 2002; 70:759–767.

16 van Meeteren L, Ruurs P, Stortelers C, Bouwman P, van Rooijen M, Pradère J, Pettit T, Wakelam M, Saulnier-Blache J, Mummery C, Moolenaar W, Jonkers J: Autotaxin, a secreted lysophospholipase D, is essential for blood vessel formation during development. *Mol Cell Biol* 2006; 26:5015–5022.

17 Nakamura K, Ohkawa R, Okubo S, Tozuka M, Okada M, Aoki S, Aoki J, Arai H, Ikeda H, Yatomi Y: Measurement of lysophospholipase D/autotaxin activity in human serum samples. *Clin Biochem* 2007; 40:274–277.

18 Tokumura A, Kanaya Y, Miyake M, Yamano S, Irahara M, Fukuzawa K: Increased production of bioactive lysophosphatidic acid by serum lysophospholipase D in human pregnancy. *Biol Reprod* 2002; 67:1386–1392.

19 Tanaka M, Kishi Y, Takanezawa Y, Kakehi Y, Aoki J, Arai H: Prostatic acid phosphatase degrades lysophosphatidic acid in seminal plasma. *FEBS Lett* 2004; 571:197–204.

20 Baumforth KR, Flavell JR, Reynolds GM, Davies G, Pettitt TR, Wei W, Morgan S, Stankovic T, Kishi Y, Arai H, Nowakova M, Pratt G, Aoki J, Wakelam MJ, Young LS, Murray PG: Induction of autotaxin by the Epstein–Barr virus promotes the growth and survival of Hodgkin's lymphoma cells. *Blood* 2005; 106:2138–2146.

21 Savaskan NE, Rocha L, Kotter MR, Baer A, Lubec G, van Meeteren LA, Kishi Y, Aoki J, Moolenaar WH, Nitsch R, Brauer AU: Autotaxin (NPP-2) in the brain: cell type-specific expression and regulation during development and after neurotrauma. *Cell Mol Life Sci* 2007; 642:230–243.

22 Kehlen A, Englert N, Seifert A, Klonisch T, Dralle H, Langner J, Hoang-Vu C: Expression, regulation and function of autotaxin in thyroid carcinomas. *Int J Cancer* 2004; 109:833–838.

23 Kawana K, Kawana Y, Schust DJ: Female steroid hormones use signal transducers and activators of transcription protein-mediated pathways to modulate the expression of T-bet in epithelial cells: a mechanism for local immune regulation in the human reproductive tract. *Mol Endocrinol* 2005; 19:2047–2059.

24 Ye X, Hama K, Contos JJA, Anliker B, Inoue A, Skinner MK, Suzuki H, Amano T, Kennedy G, Arai H, Aoki J, Chun J: LPA3-mediated lysophosphatidic acid signalling in embryo implantation and spacing. *Nature* 2005; 435:104–108.

25 Jeng YJ, Suarez VR, Izban MG, Wang HQ, Soloff MS: Progesterone- induced sphingosine kinase-1 expression in the rat uterus during pregnancy and signaling consequences. *Am J Physiol Endocrinol Metab* 2007; 292:E1110–E1121.

26 Tokumura A, Fukuzawa K, Yamada S, Tsukatani H: Stimulatory effect of lysophosphatidic acids on uterine smooth muscles of non-pregnant rats. *Arch Int Pharmacodyn Ther* 1980; 245:74–83.

27 Jeng YJ, Soloff SL, Anderson GD, Soloff MS: Regulation of oxytocin receptor expression in cultured human myometrial cells by fetal bovine serum and lysophospholipids. *Endocrinology* 2003; 144:61–68.

British Journal of Cancer (2009) 101, 145 – 148

www.bjcancer.com

The oncogenic mutation in the pleckstrin homology domain of AKT1 in endometrial carcinomas

K Shoji[1], K Oda[*,1], S Nakagawa[1], S Hosokawa[1], G Nagae[2], Y Uehara[1], K Sone[1], Y Miyamoto[1], H Hiraike[1], O Hiraike-Wada[1], T Nei[1], K Kawana[1], H Kuramoto[3], H Aburatani[2], T Yano[1] and Y Taketani[1]

[1]Department of Obstetrics and Gynecology, The University of Tokyo, 7-3-1 Hongo Bunkyo-ku, Tokyo 113-8655, Japan; [2]Genome Science Division, Research Center for Advanced Science and Technology, The University of Tokyo, 4-6-1 Komaba Meguro-ku, Tokyo 153-8904, Japan; [3]Department of Clinical Cytology, Kitasato University Graduate School of Medical Sciences, Kitasato 1-15-1 Sagamihara-shi, Kanagawa 228-8555, Japan

BACKGROUND: The phosphatidylinositol 3′-kinase (PI3K)–AKT pathway is activated in many human cancers and plays a key role in cell proliferation and survival. A mutation (E17K) in the pleckstrin homology domain of the *AKT1* results in constitutive AKT1 activation by means of localisation to the plasma membrane. The *AKT1* (E17K) mutation has been reported in some tumour types (breast, colorectal, ovarian and lung cancers), and it is of interest which tumour types other than those possess the *E17K* mutation.

METHODS: We analysed the presence of the *AKT1* (E17K) mutation in 89 endometrial cancer tissue specimens and in 12 endometrial cancer cell lines by PCR and direct sequencing.

RESULTS: We detected two *AKT1* (E17K) mutations in the tissue samples (2 out of 89) and no mutations in the cell lines. These two *AKT1* mutant tumours do not possess any mutations in *PIK3CA*, *PTEN* and *K-Ras*.

INTERPRETATION: Our results and earlier reports suggest that *AKT1* mutations might be mutually exclusive with other PI3K–AKT-activating alterations, although *PIK3CA* mutations frequently coexist with other alterations (such as *HER2*, *K-Ras* and *PTEN*) in several types of tumours.

British Journal of Cancer (2009) **101**, 145 – 148. doi:10.1038/sj.bjc.6605109 www.bjcancer.com
Published online 2 June 2009

Keywords: *AKT1*; mutation; PI3-kinase; endometrial carcinoma

The AKT serine/threonine kinases regulate diverse cellular processes, including cell survival, proliferation, invasion and metabolism (Vivanco and Sawyers, 2002). The phosphatidylinositol 3′-kinases (PI3Ks) are widely expressed lipid kinases that catalyse the production of the second messenger phosphatidylinositol 3,4,5-triphosphate (PIP3), which activates AKT by recruitment to the plasma membrane through direct contact of its pleckstrin homology (PH) domain (Stokoe *et al*, 1997; Lemmon and Ferguson, 2000). Constitutive PI3K–AKT pathway activation can result from various types of alterations in this pathway, including mutation or amplification of receptor tyrosine kinases (such as *EGFR* and *HER2*), mutation of *Ras*, mutation or amplification of *PIK3CA* (the p110α catalytic subunit of PI3K) and inactivation of the tumour suppressor gene, *PTEN* (Yuan and Cantley, 2008). In addition to amplifications in multiple AKT isoforms in pancreatic, ovarian and head and neck cancers (Engelman *et al*, 2006), a somatic missense mutation in the PH domain of *AKT1* (E17K) was identified in breast, colorectal, ovarian and lung cancers and in melanoma (Carpten *et al*, 2007; Bleeker *et al*, 2008; Davies *et al*, 2008; Malanga *et al*, 2008). However, the *AKT1* mutation has not been identified in hepatocellular, gastric and pancreatic cancers, leukemia, as well as in glioblastoma multiforme (Bleeker *et al*, 2008; Cao *et al*, 2008; Kim *et al*, 2008; Mahmoud *et al*, 2008; Mohamedali *et al*, 2008; Riener *et al*, 2008; Zenz *et al*, 2008). Further study is required to fully understand which tumour types take advantage of *Akt1* (E17K) mutations to activate the PI3K–AKT pathway.

We reported earlier that *PIK3CA* mutations frequently coexist with other PI3K-activating alterations in breast (with *HER2* and *HER3*) and endometrial cancers (with *PTEN* and *K-Ras*), and that mutant p110α combined with mutant Ras efficiently transformed immortalised human mammary epithelial cells (Oda *et al*, 2005, 2008). Frequent overlapping mutations of *K-Ras* and *PIK3CA* were also reported in colorectal cancer (Parsons *et al*, 2005). Although coexistent mutations of *AKT1* and *PIK3CA* mutations are suggested to be infrequent in breast cancer (Carpten *et al*, 2007; Bleeker *et al*, 2008), it remains to be elucidated whether *AKT1* mutations are mutually exclusive with all the other PI3K–AKT-activating alterations in various tumour types.

Endometrial cancer is one of the tumour types in which the PI3K–AKT pathway is frequently activated by alterations of various genes. The frequency of mutations for *PTEN*, *PIK3CA* and *K-Ras* in endometrial cancer is reported as 54, 28 and 11%, respectively (Yuan and Cantley, 2008). In this study, we screened 89 endometrial carcinoma specimens and 12 endometrial carcinoma cell lines for mutations in *Akt1* (E17K) and analysed whether *AKT1* mutations coexist with any mutations in *PTEN*, *PIK3CA* and *K-Ras*.

MATERIALS AND METHODS

Tumour samples and genomic DNA

Surgical samples were obtained from 89 patients with primary endometrial carcinomas who underwent resection of their tumours

*Correspondence: Dr K Oda; E-mail: katsutoshi-tky@umin.ac.jp
Received 16 February 2009; revised 21 April 2009; accepted 27 April 2009; published online 2 June 2009

at the University of Tokyo Hospital. All patients provided informed consent for the research use of their samples and the collection, and the use of tissues for this study was approved by the appropriate institutional ethics committees. Genomic DNA was extracted by a standard SDS-proteinase K procedure. Patient characteristics (histology, tumour grade and stage) are available in Supplementary Table 1. A detailed distribution of the histological subtypes was as follows; 81 (90%) endometrioid adenocarcinomas, 3 adenosquamous carcinomas, 1 clear cell carcinoma, 1 squamous cell carcinoma and 3 mixed carcinomas.

PCR and sequencing

The primer sequences and PCR conditions of exon 4 of the *AKT1* gene are forward: 5′-CACACCCAGTTCCTGCCT G-3′ and reverse: 5′-CCTGGTGGGCAAAGAGGGCT-3′. The PCR amplifications were with denaturation at 94°C for 5 min, followed by 35 cycles of 94°C for 30 s, 55°C for 30 s, 72°C for 60 s and final extension at 72°C for 10 min. The PCR conditions and the PCR primers for *PIK3CA* (exons 9 and 20), *PTEN* (exons 1–9) and *K-Ras* (exons 1 and 2) were described earlier (Minaguchi *et al*, 2001; Samuels *et al*, 2004; Oda *et al*, 2008). The PCR products were sequenced using the BigDye (Applied Biosystems, Foster City, CA, USA) terminator method on an autosequencer.

Cell lines

In this study, AN3CA, KLE, HEC-1B and RL95-2 were obtained from the American Type Culture Collection (Manassas, VA, USA) and HHUA was obtained from the RIKEN CELL BANK (Tsukuba, Japan). Ishikawa3-H-12 was a generous gift from Dr Masato Nishida (Kasumigaura Medical Center, Ibaraki, Japan). HEC-6, HEC-50B, HEC-59, HEC-88, HEC-108 and HEC-116 cell lines were also analysed in this study. The culture condition of all these cell lines was described earlier (Oda *et al*, 2008).

DNA methylation analysis

Bisulphite treatment was performed using the EZ DNA methylation kit (Zymo Research, Orange, CA, USA). As described earlier (Ehrich *et al*, 2006), we used Sequenom's MassARRAY platform to perform quantitative methylation analysis of multiple CpG sites for *PTEN* in 53 endometrial tumour specimens (Sequenom, San Diego, CA, USA). Chromosomal localisation of CpG islands for *PTEN* and the primer sequences in this study are shown in Supplementary Figure 1.

Immunohistochemistry (IHC)

Immunohistochemistry for PTEN on 4-μm tissue sections was performed and evaluated as described earlier (Minaguchi *et al*, 2007). In this study, the anti-PTEN Rabbit monoclonal antibody (138G6) (Cell Signaling, Beverly, MA, USA) was applied at a dilution of 1 : 100.

Single nucleotide polymorphism (SNP) array

Single nucleotide polymorphism array was performed in the two *AKT1* mutant tumours with tumour DNA. Experimental procedures for GeneChip were performed according to GeneChip Expression Analysis Technical Manual (Affymetrix, Santa Clara, CA, USA), using a Human mapping 50K Array Xba I (Affymetrix).

RESULTS AND DISCUSSIONS

The sequencing analysis for exon 4 of the *AKT1* gene in 89 tumour tissue samples of endometrial carcinomas showed the point mutation of G to A at nucleotide 49 (E17K) in two tissue samples (2.2%) (Figure 1). Both of the tumours were well-differentiated endometrioid adenocarcinomas with positive oestrogen receptor and progesterone receptor, suggesting that these two tumours are oestrogen dependent (corresponded to type I endometrial cancer). No mutations were detected in the 12 endometrial cancer cell lines.

Thereafter, we attempted to figure out the exclusivity of *AKT1* mutations and other PI3K–AKT-activating mutations (Supplementary Table 1). The genotypic pattern of the four genes (*PTEN*, *PIK3CA*, *K-Ras* and *AKT1*) in 97 endometrial carcinomas (85 tumour tissue samples and 12 cell lines) was shown in Table 1. Coexistence with other mutations is frequently observed in the *PIK3CA* mutant (28 of 34; 82%) and in the *K-Ras* mutant (13 out of 17; 76%) tumours, but the two *AKT1* mutant tumours do not possess any mutations in *PTEN*, *PIK3CA* and *K-Ras*. As PI3K and

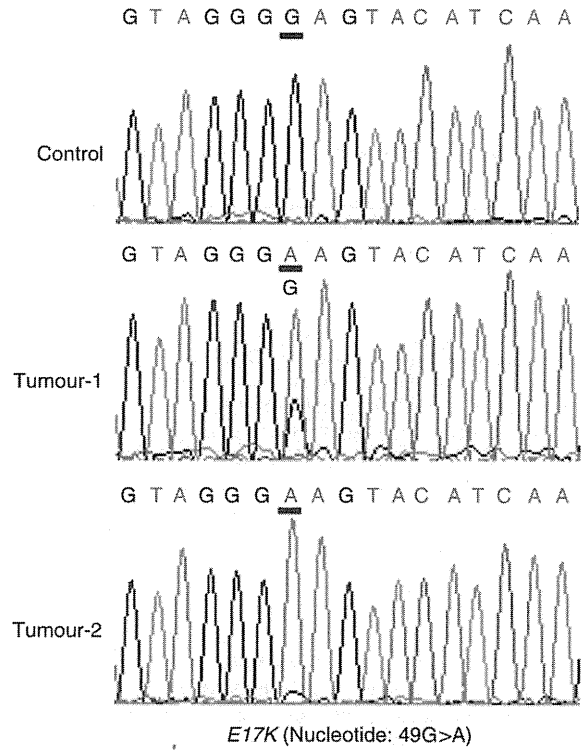

Figure 1 The sequence traces of two tumours and a normal control for exon 4 of *AKT1*. The *E17K* mutation is caused by a missense mutation (G to A) indicated. In tumour-2, the level of the mutant band (A) is much higher than that of the wild-type band (G). It is possible that this weak band is derived from DNA of normal cells and that the tumour might lose one allele at this locus.

Table 1 PI3K–AKT activating mutations and their coexistence in 97 endometrial cancers

	n (%)
Wild-type	24 (25)
AKT1 mutation alone	2 (2)
K-Ras mutation alone	4 (4)
PIK3CA mutation alone	6 (6)
PTEN mutation alone	30 (31)
Double mutations of *K-Ras* and *PIK3CA* (w/o *PTEN* mutation)	2 (2)
Double mutations of *K-Ras* and *PTEN* (w/o *PIK3CA* mutation)	3 (3)
Double mutations of *PIK3CA* and *PTEN* (w/o *K-Ras* mutation)	18 (19)
Triple mutations of *K-Ras*, *PIK3CA* and *PTEN*	8 (8)

PI3K, phosphatidylinositol 3′-kinase. Wild-type, no mutations in *PTEN*, *PIK3CA*, *K-Ras* and *AKT1*.

PTEN are competitive for PIP3 production, the *PIK3CA* mutation might require another upstream input or PTEN loss itself to fully activate the PI3K–AKT pathway. As AKT1 (E17K) functions downstream of PTEN and shows constitutive localisation to the plasma membrane in the absence of serum stimulation (Carpten *et al*, 2007), mutant *AKT1* (E17K) alone might be sufficient for complete activation of this pathway.

We also analysed DNA methylation and protein expression of PTEN, as hypermethylation and loss of heterozygosity (LOH) are other mechanisms to inactivate PTEN (Teng *et al*, 1997; Blanco-Aparicio *et al*, 2007). Quantitative analysis of DNA methylation using Sequenom's MassARRAY platform did not find promoter hypermethylation of *PTEN* in all the 53 samples that were examined (Supplementary Figure 2 and Supplementary Table 2), including the two *AKT1* mutant tumours. Although *PTEN* methylation had been reported in 18% of endometrial carcinomas (Salvesen *et al*, 2001), Zysman *et al* (2002) suggested that the pseudogene on chromosome 9 (Genbank accession number: AF040103), not *PTEN*, is predominantly methylated in endometrial carcinomas. In IHC, both tumours with the *AKT1* mutation were stained positively for PTEN in the cytoplasm, whereas all the four tumours with multiple frameshift mutations in *PTEN* were stained negatively (Supplementary Figure 3). We evaluated the chromosomal imbalances in the two *AKT1* mutant tumours, using SNP array (with more than 50 000 SNPs). Single nucleotide polymorphism array analysis showed that the two *AKT1* mutant tumours do not show copy number changes in the locus of *PTEN* (10q23.1) (data not shown). These data also support the fact that *AKT1* mutations are mutually exclusive with PTEN inactivation.

We found multiple *PTEN* mutations in 13 out of 85 clinical specimens and in 8 out of 12 endometrial cell lines (Supplementary Table 1), whereas LOH of *PTEN* was reported approximately at 30% in endometrial carcinomas (Toda *et al*, 2001). Thus, biallelic *PTEN* inactivation might be achieved through either biallelic mutations or monoallelic mutation with LOH in endometrial carcinomas. Considering the correlation between *PTEN* mutations and microsatellite instability (MSI) in endometrial carcinomas (Bilbao *et al*, 2006), it would be of interest to analyse whether *AKT1* and the other mutations in the PI3K pathway genes are also associated with MSI.

To date, *AKT1* (E17K) mutations have been reported in breast (25 out of 427; 5.9%), colorectal (4 out of 243; 1.6%), lung (4 out of 636; 0.6%) and ovarian cancers (1 out of 130; 0.8%) and in melanoma (1 out of 202; 0.5%). Breast, colorectal and endometrial cancers are the tumour types that frequently possess *PIK3CA* mutations (Campbell *et al*, 2004; Samuels *et al*, 2004; Oda *et al*, 2005). In lung cancer, the *AKT1* mutation was detected only in squamous cell carcinomas and not in any adenocarcinomas, which is in agreement with the higher incidence of *PIK3CA* mutations or amplifications in squamous cell carcinomas than adenocarcinomas (Kawano *et al*, 2006, 2007; Malanga *et al*, 2008). These data suggest that the *AKT1* mutation might occur in a tissue-specific manner and is more associated with the tumour types with frequent *PIK3CA* alterations.

ACKNOWLEDGEMENTS

We thank Kaoru Nakano, Hiroko Meguro, Shingo Yamamoto, Akira Tsuchiya and GLab Pathology Center Co., Ltd. for their technical support. We thank Dr Masato Nishida for Ishikawa3-H-12 cell line. This work was supported by KAKENHI, the Grant-in-aid for Scientific Research (C) in Japan, number 19599005 (to K Oda).

Supplementary Information accompanies the paper on British Journal of Cancer website (http://www.nature.com/bjc)

REFERENCES

Bilbao C, Rodriguez G, Ramirez R, Falcon O, Leon L, Chirino R, Rivero JF, Falcon Jr O, Diaz Chico BN, Diaz Chico JC, Perucho M (2006) The relationship between microsatellite instability and PTEN gene mutations in endometrial cancer. *Int J Cancer* **119:** 563–570

Blanco-Aparicio C, Renner O, Leal JF, Carnero A (2007) PTEN, more than the AKT pathway. *Carcinogenesis* **28:** 1379–1386

Bleeker FE, Felicioni L, Buttitta F, Lamba S, Cardone L, Rodolfo M, Scarpa A, Leenstra S, Frattini M, Barbareschi M, Grammastro MD, Sciarrotta MG, Zanon C, Marchetti A, Bardelli A (2008) AKT1(E17K) in human solid tumours. *Oncogene* **27:** 5648–5650

Campbell IG, Russell SE, Choong DY, Montgomery KG, Ciavarella ML, Hooi CS, Cristiano BE, Pearson RB, Phillips WA (2004) Mutation of the PIK3CA gene in ovarian and breast cancer. *Cancer Res* **64:** 7678–7681

Cao Z, Song JH, Kim CJ, Cho YG, Kim SY, Nam SW, Lee JY, Park WS (2008) Absence of E17K mutation in the pleckstrin homology domain of AKT1 in gastrointestinal and liver cancers in the Korean population. *APMIS* **116:** 530–533

Carpten JD, Faber AL, Horn C, Donoho GP, Briggs SL, Robbins CM, Hostetter G, Boguslawski S, Moses TY, Savage S, Uhlik M, Lin A, Du J, Qian YW, Zeckner DJ, Tucker Kellogg G, Touchman J, Patel K, Mousses S, Bittner M, Schevitz R, Lai MH, Blanchard KL, Thomas JE (2007) A transforming mutation in the pleckstrin homology domain of AKT1 in cancer. *Nature* **448:** 439–444

Davies MA, Stemke Hale K, Tellez C, Calderone TL, Deng W, Prieto VG, Lazar AJ, Gershenwald JE, Mills GB (2008) A novel AKT3 mutation in melanoma tumours and cell lines. *Br J Cancer* **99:** 1265–1268

Ehrich M, Field JK, Liloglou T, Xinarianos G, Oeth P, Nelson MR, Cantor CR, van den Boom D (2006) Cytosine methylation profiles as a molecular marker in non-small cell lung cancer. *Cancer Res* **66:** 10911–10918

Engelman JA, Luo J, Cantley LC (2006) The evolution of phosphatidylinositol 3-kinases as regulators of growth and metabolism. *Nat Rev Genet* **7:** 606–619

Kawano O, Sasaki H, Endo K, Suzuki E, Haneda H, Yukiue H, Kobayashi Y, Yano M, Fujii Y (2006) PIK3CA mutation status in Japanese lung cancer patients. *Lung Cancer* **54:** 209–215

Kawano O, Sasaki H, Okuda K, Yukiue H, Yokoyama T, Yano M, Fujii Y (2007) PIK3CA gene amplification in Japanese non-small cell lung cancer. *Lung Cancer* **58:** 159–160

Kim MS, Jeong EG, Yoo NJ, Lee SH (2008) Mutational analysis of oncogenic AKT E17K mutation in common solid cancers and acute leukaemias. *Br J Cancer* **98:** 1533–1535

Lemmon MA, Ferguson KM (2000) Signal-dependent membrane targeting by pleckstrin homology (PH) domains. *Biochem J* **350**(Pt 1): 1–18

Mahmoud IS, Sughayer MA, Mohammad HA, Awidi AS, EL-Khateeb MS, Ismail SI (2008) The transforming mutation E17K/AKT1 is not a major event in B-cell-derived lymphoid leukaemias. *Br J Cancer* **99:** 488–490

Malanga D, Scrima M, De Marco C, Fabiani F, De Rosa N, De Gisi S, Malara N, Savino R, Rocco G, Chiappetta G, Franco R, Tirino V, Pirozzi G, Viglietto G (2008) Activating E17K mutation in the gene encoding the protein kinase AKT1 in a subset of squamous cell carcinoma of the lung. *Cell Cycle* **7:** 665–669

Minaguchi T, Nakagawa S, Takazawa Y, Nei T, Horie K, Fujiwara T, Osuga Y, Yasugi T, Kugu K, Yano T, Yoshikawa H, Taketani Y (2007) Combined phospho-Akt and PTEN expressions associated with post-treatment hysterectomy after conservative progestin therapy in complex atypical hyperplasia and stage Ia, G1 adenocarcinoma of the endometrium. *Cancer Lett* **248:** 112–122

Minaguchi T, Yoshikawa H, Oda K, Ishino T, Yasugi T, Onda T, Nakagawa S, Matsumoto K, Kawana K, Taketani Y (2001) PTEN mutation located only outside exons 5, 6, and 7 is an independent predictor of favorable survival in endometrial carcinomas. *Clin Cancer Res* **7:** 2636–2642

Mohamedali A, Lea NC, Feakins RM, Raj K, Mufti GJ, Kocher HM (2008) AKT1 (E17K) mutation in pancreatic cancer. *Technol Cancer Res Treat* **7:** 407–408

Oda K, Okada J, Timmerman L, Rodriguez Viciana P, Stokoe D, Shoji K, Taketani Y, Kuramoto H, Knight ZA, Shokat KM, McCormick F (2008) PIK3CA cooperates with other phosphatidylinositol 3′-kinase pathway mutations to effect oncogenic transformation. *Cancer Res* **68:** 8127–8136

Oda K, Stokoe D, Taketani Y, McCormick F (2005) High frequency of coexistent mutations of PIK3CA and PTEN genes in endometrial carcinoma. *Cancer Res* **65:** 10669–10673

Parsons DW, Wang TL, Samuels Y, Bardelli A, Cummins JM, DeLong L, Silliman N, Ptak J, Szabo S, Willson JK, Markowitz S, Kinzler KW, Vogelstein B, Lengauer C, Velculescu VE (2005) Colorectal cancer: mutations in a signalling pathway. *Nature* **436:** 792

Riener MO, Bawohl M, Clavien PA, Jochum W (2008) Analysis of oncogenic AKT1 p.E17K mutation in carcinomas of the biliary tract and liver. *Br J Cancer* **99:** 836

Salvesen HB, MacDonald N, Ryan A, Jacobs IJ, Lynch ED, Akslen LA, Das S (2001) PTEN methylation is associated with advanced stage and microsatellite instability in endometrial carcinoma. *Int J Cancer* **91:** 22–26

Samuels Y, Wang Z, Bardelli A, Silliman N, Ptak J, Szabo S, Yan H, Gazdar A, Powell SM, Riggins GJ, Willson JK, Markowitz S, Kinzler KW, Vogelstein B, Velculescu VE (2004) High frequency of mutations of the PIK3CA gene in human cancers. *Science* **304:** 554

Stokoe D, Stephens LR, Copeland T, Gaffney PR, Reese CB, Painter GF, Holmes AB, McCormick F, Hawkins PT (1997) Dual role of phosphatidylinositol-3,4,5-trisphosphate in the activation of protein kinase B. *Science* **277:** 567–570

Teng DH, Hu R, Lin H, Davis T, Iliev D, Frye C, Swedlund B, Hansen KL, Vinson VL, Gumpper KL, Ellis L, El Naggar A, Frazier M, Jasser S, Langford LA, Lee J, Mills GB, Pershouse MA, Pollack RE, Tornos C, Troncoso P, Yung WK, Fujii G, Berson A, Steck PA, Bookstein R, Bolen JB, Tavtigian SV (1997) MMAC1/PTEN mutations in primary tumor specimens and tumor cell lines. *Cancer Res* **57:** 5221–5225

Toda T, Oku H, Khaskhely NM, Moromizato H, Ono I, Murata T (2001) Analysis of microsatellite instability and loss of heterozygosity in uterine endometrial adenocarcinoma. *Cancer Genet Cytogenet* **126:** 120–127

Vivanco I, Sawyers CL (2002) The phosphatidylinositol 3-Kinase AKT pathway in human cancer. *Nat Rev Cancer* **2:** 489–501

Yuan TL, Cantley LC (2008) PI3K pathway alterations in cancer: variations on a theme. *Oncogene* **27:** 5497–5510

Zenz T, Dohner K, Denzel T, Dohner H, Stilgenbauer S, Bullinger L (2008) Chronic lymphocytic leukaemia and acute myeloid leukaemia are not associated with AKT1 pleckstrin homology domain (E17K) mutations. *Br J Haematol* **141:** 742–743

Zysman MA, Chapman WB, Bapat B (2002) Considerations when analyzing the methylation status of PTEN tumor suppressor gene. *Am J Pathol* **160:** 795–800

Effect of Progesterone on HLA-E Gene Expression in JEG-3 Choriocarcinoma Cell Line

Zhongying Huang[1,2], Hironobu Hyodo[1], Tomoyuki Fujii[1], Takeshi Nagamatsu[1], Junko Matsumoto[1], Kei Kawana[1], Takahiro Yamashita[1], Toshiharu Yasugi[1], Shiro Kozuma[1], Yuji Taketani[1]

[1]Department of Obstetrics and Gynecology, The University of Tokyo, Tokyo, Japan;
[2]Department of Obstetrics and Gynecology, West China Second Hospital, Sichuan University, Chengdu, China

Keywords
human leukocyte antigen-E, JEG-3, progesterone, trophoblast

Correspondence
Hironobu Hyodo, Department of Obstetrics and Gynecology, The University of Tokyo, 7-3-1 Hongo, Bunkyo, Tokyo 113-8655, Japan.
E-mail: hyodo-tky@umin.ac.jp

Submitted November 22, 2008;
accepted December 29, 2008.

Citation
Huang Z, Hyodo H, Fujii T, Nagamatsu T, Matsumoto J, Kawana K, Yamashita T, Yasugi T, Kozuma S, Taketani Y. Effect of progesterone on HLA-E gene expression in JEG-3 choriocarcinoma cell line. Am J Reprod Immunol 2009; 61: 221–226

doi:10.1111/j.1600-0897.2008.00684.x

Problem
Among class Ib human leukocyte antigen (HLA) molecules, HLA-E is known to be a major ligand of CD94/NKG2 receptor on natural killer (NK) cells, and to play a pivotal role in recognition of extravillous trophoblasts (EVTs) by maternal immune cells. However, it is scarcely known how HLA-E expression is regulated in EVTs.

Method of study
In this study, we investigated whether progesterone, an essential hormone in maintaining pregnancy, regulated HLA-E expression in EVT-like cell line, JEG-3. HLA-E mRNA amount in cultured JEG-3 cells was assessed by real-time PCR and cell-surface HLA-E protein was analyzed by flowcytometry.

Results
Real-time PCR showed 3.5-fold increase 1 hour after the addition of 1000 ng/ml progesterone. This response was dimished by the addition of RU486, an antagonist for progesterone receptor. Flowcytometry indicated that 1000 ng/ml progesterone slightly enhanced HLA-E expression on the surface of JEG-3.

Conclusion
These results suggest that progesterone up-regulates HLA-E expression in JEG-3 cells through the pathway mediated by progesterone receptor. Our findings might give a new insight into immunomodulatory function of progesterone at fetomaternal interface.

Introduction

In human placenta, expression of human leukocyte antigen (HLA) molecules on trophoblasts is highly restricted. The interaction between HLA molecules on trophoblasts and the corresponding receptors on decidual lymphocytes is considered to be an immunological key for successful pregnancy. Extravillous trophoblasts (EVTs) come into direct contact with maternal immune cells in their migrating process into the decidua. EVTs do not express HLA class II and class Ia molecules except for HLA-C.[1] Instead, they express low polymorphic class Ib molecules such as HLA-E, -F and -G.[2,3] Among class Ib molecules on trophoblasts, HLA-G has been most extensively studied about its molecular distribution in placenta as well as its function based on the hypothesis that HLA-G has specialized function in the immunological tolerance to fetus because of the unique localization restricted to fetomaternal interface in placenta. On

the other hand, recent works also have progressively revealed the biological profile of HLA-E. Although the endogenous expression of HLA-E is confirmed in the vast range of cells and tissues,[4] the degree of cell surface expression is dependent on the availability of nonamer peptide derived from other HLA class I signal sequences.[5–8] In case of EVTs, the cell surface expression of HLA-E is implied to be supported by the supply of leader peptides of HLA-G and -C. Uterine natural killer (uNK) cells possibly respond to HLA-E on EVTs mediated by the inhibitory receptor, CD94/NKG2A. This immunological interaction could induce significant modulation in fetomaternal immunological paradigm.

Progesterone has been considered to be an essential hormone in maintaining pregnancy although its function is not fully elucidated. Among its fundamental roles, the action as an immunomodulator has been reported. Progesterone reduces the cytotoxic activity of NK cells[9] and T-cells,[10] and also modulates T helper 1 and T helper 2 balance.[11,12] Recently, progesterone has been reported to enhance the expression of HLA-G on trophoblasts.[13] Given that, HLA-G has specialized immunological function at the interface between mother and fetus, progesterone might contribute to the maternal immunological tolerance to the fetus through the regulation of HLA-G expression on trophoblasts. However, the influence of progesterone on HLA-E, another HLA class Ib molecule that affects the immune interaction between mother and fetus, has not been elucidated. In this study, we tried to investigate the effect of progesterone on HLA-E expression in trophoblasts at mRNA and protein level by using JEG-3 choriocarcinoma cell line.

Materials and methods

Cell Lines and Cultures

Human choriocarcinoma cell line JEG-3, was obtained from American Type Culture Collection (ATCC, Rockville, MD, USA) and maintained in RPMI 1640 (Sigma, St Louis, MO, USA) supplemented with 10% heat-inactivated fetal bovine serum (FBS) and antibiotics/antimycotics (GibcoBRL, Grand Island, NY, USA) at 37°C in a humidified 5% CO_2 atmosphere. Cells were seeded at a concentration of 1×10^5/mL. When cells were grown to approximately 60% confluence, we replaced media with serum-free RPMI1640. After 24 hr, the culture media were refreshed again and progesterone (10, 100, 1000 ng/mL) was added to the culture dishes assigned to each assay. In the case of inhibition assay, RU486 (1000 ng/mL) (Sigma) was concomitantly supplemented to the culture with progesterone. Progesterone and RU486 were dissolved into 99.5% ethanol and prepared in 10, 100 or 1000 μg/mL stock. 2 μL of the stock solution was added to 2 mL of culture media.

Reverse-transcriptase Reaction and Real-time Polymerase Chain Reaction

Total RNA of JEG-3 cells was extracted from the cells using RNAeasy Mini Kit (Qiagen, Hilden, Germany) and was reverse-transcribed with the ReverTraAce kit (Toyobo, Osaka, Japan) according to the manufacturer's instruction. Real-time polymerase chain reaction (PCR) was carried out using iCycler iQ Real-time PCR Detection System (Bio-Rad, Hercules, CA, USA). The sequences of gene-specific primers are summarized in Table I.[14] PCR was performed in a 20 μL volume containing aliquots of diluted cDNA, 0.5 μM primers, 2.3 mM $MgCl_2$ and 0.3 μL 100X SYBR Green I DNA master mixture (Roche Diagnostics, Lewes, UK). For negative control, water was used instead of the target cDNA template. After 3 min denaturation at 95°C, 40 cycles of amplification were carried out: 95°C denaturation for 20 s, 56°C annealing for 30 s, and 72°C extension for 30 s. Beta-actin was used as an internal control in each sample to compensate the variations in quantities and qualities among cDNA samples. The amount of HLA-E mRNA was normalized against that of beta-actin. The amplification specificity of PCR prod-

Table I Primers for Real-Time PCR of HLA-E

Primer	Forward primers	Reverse primers	Size
HLA-E	5′-GGGACACCGCACAGATTTT-3′	5′-CTCAGAGGCATCATTTGACTTTT-3′	254
Beta-actin	5′-AAGGCCAACCGCGAGAA-3′	5′-CCTCGTAGATGGGCACA-3′	166

ucts was confirmed by melting curve analysis and electrophoresis on a 2% agarose gel.

Flow Cytometric Analysis

Cultured JEG-3 cells were detached from culture plates with 0.05% trypsin-EDTA (GibcoBRL) after different culture periods. Cells were washed with PBS containing 1% FBS and 0.1% NaN_3 and incubated with saturating concentrations of anti-HLA-E-specific monoclonal antibody 3D12[5] (provided by Dr Daniel E Geraghty, Fred Hutchinson Cancer Research Center, Seattle, WA, USA), or mouse isotype-matched IgG1 (Dako, Glostrup, Denmark) for 30 min at 4°C. After washing three times to remove unbound antibody, the cells were incubated with fluorescein isothiocyanate-conjugated anti-mouse IgG $F(ab')_2$ rabbit IgG (Dako) for 30 min at 4°C. The cells were subsequently resuspended in PBS containing 1% paraformaldehyde for detection. Fifty thousand cells were detected for each sample using a Coulter EPICSR XL flow cytometer (Beckman Coulter, Tokyo, Japan) and the data analysis was carried out using EXPO32™ software (Beckman Coulter).

Statistics

Statistical analysis was carried out using Wilcoxon test for pair-matched samples. When P value was less than 0.05, the difference was regarded as statistically significant.

Results

Effect of Progesterone on HLA-E mRNA Expression

Human leukocyte antigen-E mRNA amount of JEG-3 cells treated with 1000 ng/mL of progesterone increased up to 3.5-fold of that of control ($P < 0.05$) at 1 hr culture, while no significant increase was observed at 30 min, 2, 3 and 4 hr (Fig. 1a). Addition of 10 or 100 ng/mL of progesterone did not show any change of HLA-E mRNA amount at any time point of culture from 30 min to 4 hr. RU486, an antagonist for progesterone receptor, added to the culture medium concomitantly with 1000 ng/mL of progesterone, diminished the effect of progesterone on HLA-E mRNA amount at 1 hr (Fig. 1b). These results indicated that progesterone increased HLA-E

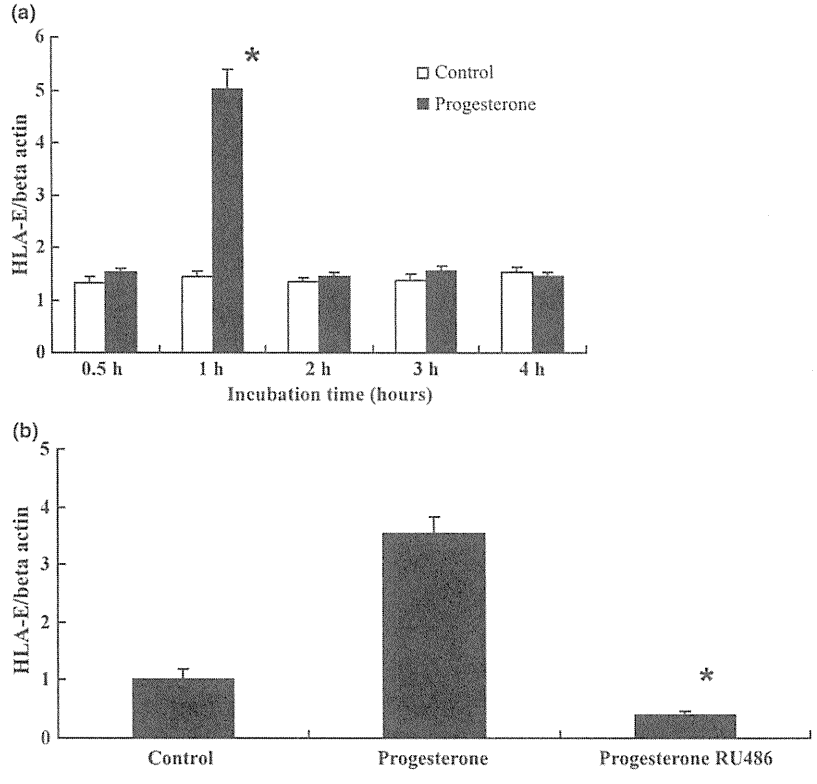

Fig. 1 The mRNA amount of HLA-E in JEG-3 cells was analyzed by real-time PCR. (a) The mRNA amount with or without progesterone was examined at different culture time (0.5, 1, 2, 3, 4 hours). In each histogram, values with progesterone are demonstrated as black columns and without progesterone as white columns. (b) The mRNA amount was examined at 1 hour culture with progesterone, both with progesterone and concomitant RU486, and without supplementation. Data are shown with standard error bar. Star mark shows there is significant difference.

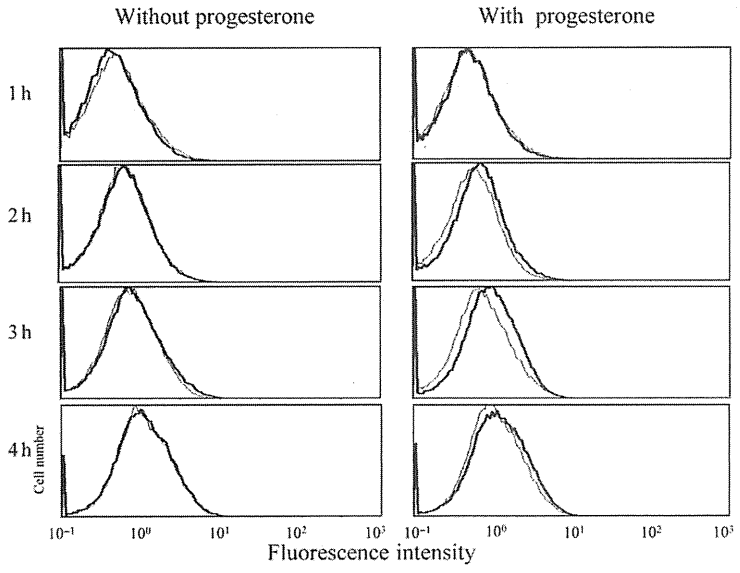

Fig. 2 Cell surface HLA-E protein expression on JEG-3 cells cultured with or without progesterone was analysed by flowcytometry using 3D12 at different culture time (1, 2, 3, 4 hours). In each histogram, values for 3D12 are demonstrated as a bold line and the negative control values as a dotted line.

mRNA expression in JEG-3 cells and RU486 diminished it.

Effect of Progesterone on Cell Surface HLA-E Protein Expression

Cell surface protein expression of HLA-E on JEG-3 cells treated with 1000 ng/mL of progesterone was investigated at several time points in culture by employing flow cytometric assay with anti-HLA-E monoclonal antibody, 3D12. The fluorescence intensity of progesterone-treated JEG-3 cells for 3D12 was slightly stronger than the control cells at 2, 3 and 4 hr (Fig. 2), indicating that progesterone slightly increased cell-surface expression of HLA-E on cultured JEG-3 cells.

Discussion

Human leukocyte antigen expression pattern of JEG-3 cells, a trophoblast-derived choriocarcinoma cell line, is so similar to that of EVTs in human placenta[15] that JEG-3 can be regarded as an *in vitro* model of EVTs to investigate the effect of progesterone on HLA expression on them.

The most outstanding finding in this study was that progesterone upregulated HLA-E mRNA expression in JEG-3 cells. This is the first demonstration that expression of HLA-E is controlled by steroid hormone. A significant mRNA increase was observed only at 1 hr in time course, indicating that the effect of progesterone was immediate and temporal. This finding is congruent with the previous report that direct activation of gene expression through steroid hormone receptor usually occurs within 1 through 4 hr.[16]

We further demonstrated that RU486 antagonized the reaction concerning HLA-E mRNA caused by progesterone, suggesting that the increase in HLA-E mRNA observed in progesterone treated cells was mediated by progesterone receptor (PR). In general, PR activated by progesterone starts to act as a transcription factor binding to progesterone response element (PRE) sequence in the promoter of target genes.[17] As no evidence showing that HLA-E gene promoter contains PRE sequence is currently available, further investigation is needed to elucidate the molecular pathway connecting PR activation and increase of HLA-E mRNA.

In this study, progesterone slightly induced the cell surface expression of HLA-E in JEG-3 cells, while no cell surface expression was detected without progesterone. One simple speculation is that the increase in HLA-E mRNA caused by progesterone contributed to intracellular amount of HLA-E protein, then directly leading to the increase in HLA-E cell surface expression. As previously reported, the surface expression of HLA-E in human trophoblasts may depend mainly on the expression of HLA-G and HLA-C, which provide nonamer peptides required for surface expression of HLA-E.[1,6,18] Considering this, the leader sequence peptide derived from

HLA-G gene product, which is reported to be enhanced by progesterone at mRNA and protein level,[13] might be another factor involved in the increased cell surface expression of HLA-E.

Human placenta daily secretes abundant progesterone up to a level of 300 mg.[19] Progesterone acts as an immunomodulator in pregnancy by blocking cytotoxic T-cell activity,[10] and suppressing NK cell activity.[9] However, according to the previous studies, PR mRNA is absent both in decidual NK cells,[20] and in peripheral blood mononuclear cells.[21] It is therefore unlikely that progesterone has direct influence on these cells. This study revealed that progesterone upregulated HLA-E gene expression, suggesting the reported progesterone effect on NK cell activity may partly be mediated by the modulation of HLA-E expression.

Uterine NK cells express high level of HLA-E specific receptor, CD94/NKG2 family molecules,[2] and besides, inhibitory CD94/NKG2A receptor binds to HLA-E with higher affinity than activating CD94/NKG2C receptor.[6,22] In the light of these facts, we can hypothesize that the increase in cell surface HLA-E expression on trophoblasts induced by progesterone may result in the suppression of the cytotoxic NK cell activity through the interaction with CD94/NKG2A receptor.

In summary, we demonstrated that progesterone upregulated HLA-E expression at mRNA level, and increased cell surface HLA-E expression in JEG-3. Although further investigation is required to see whether this reaction observed here also occurs in trophoblasts in placenta, our findings might give a new clue to the immunological mechanism supporting placental development.

References

1 King A, Burrows TD, Hiby SE, Bowen JM, Joseph S, Verma S, Lim PB, Gardner L, Le P, Ziegler A, Uchanska-Ziegler B, Loke YW: Surface expression of HLA-C antigen by human extravillous trophoblast. *Placenta* 2000; 21:376–387.

2 King A, Allan DS, Bowen M, Powis SJ, Joseph S, Verma S, Hiby SE, McMichael AJ, Loke YW, Braud VM: HLA-E is expressed on trophoblast and interacts with CD94/CDNKG2 receptors on decidual NK cells. *Eur J Immunol* 2000; 30:1623–1631.

3 Ishitani A, Sageshima N, Lee N, Dorofeeva N, Hatake K, Marquardt H, Geraghty DE: Protein expression and peptide binding suggest unique and interacting functional roles for HLA-E, F, and G in maternal-placental immune recognition. *J Immunol* 2003; 171:1376–1384.

4 Koller BH, Geraghty DE, Shimizu Y, DeMars R, Orr HT: HLA-E. A novel HLA class I gene expressed in resting T lymphocytes. *J Immunol* 1988; 141:897–904.

5 Lee N, Llano M, Carretero M, Ishitani A, Navarro F, Lopez-Botet M, Geraghty DE: HLA-E is a major ligand for the natural killer inhibitory receptor CD94/NKG2A. *Proc Natl Acad Sci USA* 1998; 95:5199–5204.

6 Llano M, Lee N, Navarro F, Garcia P, Albar JP, Geraghty DE, Lopez-Botet M: HLA-E-bound peptides influence recognition by inhibitory and triggering CD94/NKG2 receptors: preferential response to an HLA-G-derived nonamer. *Eur J Immunol* 1998; 28:2854–2863.

7 Borrego F, Ulbrecht M, Weiss EH, Coligan JE, Brooks AG: Recognition of human histocompatibility leukocyte antigen (HLA)-E complexed with HLA class I signal sequence-derived peptides by CD94/NKG2 confers protection from natural killer cell-mediated lysis. *J Exp Med* 1998; 187:813–818.

8 Navarro F, Llano M, Bellon T, Colonna M, Geraghty DE, Lopez-Botet M: The ILT2 (LIR1) and CD94/NKG2A NK cell receptors respectively recognize HLA-G1 and HLA-E molecules co-expressed on target cells. *Eur J Immunol* 1999; 29:277–283.

9 Hansen KA, Opsahl MS, Nieman LK, Baker JR Jr, Klein TA: Natural killer cell activity from pregnant subjects is modulated by RU 486. *Am J Obstet Gynecol* 1992; 166:87–90.

10 Mannel DN, Falk W, Yron I: Inhibition of murine cytotoxic T cell responses by progesterone. *Immunol Lett* 1990; 26:89–94.

11 Piccinni MP, Scaletti C, Maggi E, Romagnani S: Role of hormone-controlled Th1- and Th2-type cytokines in successful pregnancy. *J Neuroimmunol* 2000; 109:30–33.

12 Miyaura H, Iwata M: Direct and indirect inhibition of Th1 development by progesterone and glucocorticoids. *J Immunol* 2002; 168:1087–1094.

13 Yie SM, Li LH, Li GM, Xiao R, Librach CL: Progesterone enhances HLA-G gene expression in JEG-3 choriocarcinoma cells and human cytotrophoblasts in vitro. *Hum Reprod* 2006; 21:46–51.

14 Malmberg KJ, Levitsky V, Norell H, de Matos CT, Carlsten M, Schedvins K, Rabbani H, Moretta A, Söderström K, Levitskaya J, Kiessling R: IFN-gamma protects short-term ovarian carcinoma cell lines from CTL lysis via a CK94/NKG2A-dependent mechanism. *J Clin Invest* 2002; 110:1515–1523.

15 Gobin SJ, Wilson L, Keijsers V, Van den Elsen PJ: Antigen processing and presentation by human trophoblast-derived cell lines. *J Immunol* 1997; 158:3587–3592.
16 Landers JP, Spelsberg TC: New concepts in steroid hormone action: transcription factors, proto-oncogenes, and the cascade model for steroid regulation of gene expression. *Crit Rev Eukaryot Gene Expr* 1992; 2:19–63.
17 Shanker YG, Rao AJ: Progesterone receptor expression in the human placenta. *Mol Hum Reprod* 1999; 5:481–486.
18 Bhalla A, Stone PR, Liddell HS, Zanderigo A, Chamley LW: Comparison of the expression of human leukocyte antigen (HLA)-G and HLA-E in women with normal pregnancy and those with recurrent miscarriage. *Reproduction* 2006; 131:583–589.
19 Ben-Zimra M, Koler M, Melamed-Book N, Arensburg J, Payne AH, Orly J: Uterine and placental expression of steroidogenic genes during rodent pregnancy. *Mol Cell Endocrinol* 2002; 187:223–231.
20 Henderson TA, Saunders PT, Moffett-King A, Groome NP, Critchley HO: Steroid receptor expression in uterine natural killer cells. *J Clin Endocrinol Metab* 2003; 88:440–449.
21 Schust DJ, Anderson DJ, Hill JA: Progesterone-induced immunosuppression is not mediated through the progesterone receptor. *Hum Reprod* 1996; 11:980–985.
22 Kaiser BK, Barahmand-Pour F, Paulsene W, Medley S, Geraghty DE, Strong RK: Interactions between NKG2x immunoreceptors and HLA-E ligands display overlapping affinities and thermodynamics. *J Immunol* 2005; 174:2878–2884.

American Journal of Reproductive Immunology **61** (2009) 221–226

JOURNAL OF VIROLOGY, Nov. 2010, p. 11614–11623 Vol. 84, No. 22
0022-538X/10/$12.00 doi:10.1128/JVI.01053-10

CD1d, a Sentinel Molecule Bridging Innate and Adaptive Immunity, Is Downregulated by the Human Papillomavirus (HPV) E5 Protein: a Possible Mechanism for Immune Evasion by HPV[▽]

Shiho Miura,[1] Kei Kawana,[1]* Danny J. Schust,[2] Tomoyuki Fujii,[1] Terufumi Yokoyama,[3] Yuki Iwasawa,[1] Takeshi Nagamatsu,[1] Katsuyuki Adachi,[1] Ayako Tomio,[1] Kensuke Tomio,[1] Satoko Kojima,[1] Toshiharu Yasugi,[1] Shiro Kozuma,[1] and Yuji Taketani[1]

Department of Obstetrics and Gynecology, Faculty of Medicine, University of Tokyo, 7-3-1 Hongo, Bunkyo-ku, Tokyo 113-8655, Japan[1]; Division of Reproductive Endocrinology and Fertility, Department of Obstetrics, Gynecology, and Women's Health, University of Missouri School of Medicine, Columbia Regional Hospital, 402 Keene Street, Third Floor, Columbia, Missouri 65201[2]; and GENOLAC BL Corp. 503, Okinawa Industry Support Center, 1831-1, Oroku, Naha, Okinawa 901-0152, Japan[3]

Received 16 May 2010/Accepted 20 August 2010

CD1d and CD1d-restricted natural killer T (NKT) cells serve as a natural bridge between innate and adaptive immune responses to microbes. CD1d downregulation is utilized by a variety of microbes to evade immune detection. We demonstrate here that CD1d is downregulated in human papillomavirus (HPV)-positive cells *in vivo* and *in vitro*. CD1d immunoreactivity was strong in HPV-negative normal cervical epithelium but absent in HPV16-positive CIN1 and HPV6-positive condyloma lesions. We used two cell lines for *in vitro* assay; one was stably CD1d-transfected cells established from an HPV-negative cervical cancer cell line, C33A (C33A/CD1d), and the other was normal human vaginal keratinocyte bearing endogenous CD1d (Vag). Flow cytometry revealed that cell surface CD1d was downregulated in both C33A/CD1d and Vag cells stably transfected with HPV6 E5 and HPV16 E5. Although the steady-state levels of CD1d protein decreased in both E5-expressing cell lines compared to empty retrovirus-infected cells, CD1d mRNA levels were not affected. Confocal microscopy demonstrated that residual CD1d was not trafficked to the E5-expressing cell surface but colocalized with E5 near the endoplasmic reticulum (ER). In the ER, E5 interacted with calnexin, an ER chaperone known to mediate folding of CD1d. CD1d protein levels were rescued by the proteasome inhibitor, MG132, indicating a role for proteasome-mediated degradation in HPV-associated CD1d downregulation. Taken together, our data suggest that E5 targets CD1d to the cytosolic proteolytic pathway by inhibiting calnexin-related CD1d trafficking. Finally, CD1d-mediated production of interleukin-12 from the C33A/CD1d cells was abrogated in both E5-expressing cell lines. Decreased CD1d expression in the presence of HPV E5 may help HPV-infected cells evade protective immunological surveillance.

There are approximately 100 identified genotypes (types) of human papillomavirus (HPV). Over 40 of these are classified as genital HPV subtypes that invade the reproductive organs, including the uterine cervix, vaginal wall, vulva, and penis. Genital HPV types are further subclassified into high-risk types that are commonly associated with cervical cancer and low-risk types that cause noninvasive condyloma acuminata. Although exact classification varies among researchers, subtypes 16, 18, 31, 33, 35, 39, 45, 51, 52, 56, 58, 66, and 68 are typically classified as high risk and subtypes 6, 11, 40, 42, 43, 44, 54, 61, and 72 as low risk (44). Genital HPV infection involves short-term virus proliferation, followed by the long-term latent presence of a small number of copies of the viral genome within the basal cells of the genital epithelium (44). Infections with high-risk HPV subtypes result in progression to genital tract cancers (most commonly cervical) in only a small percentage of infected women and typically after a long latency period. A high percentage of high-risk HPV DNA-positive infected women resolve their infections during the proliferative phase and thereby clear the virus or progress to latency with undetectable HPV DNA levels. The clearance of viral DNA is often accomplished through activation of the host immune system against viral antigen (19), and chronic immune suppression represents a risk factor for viral DNA persistence and benign and/or neoplastic lesion progression (23).

Completion of the HPV life cycle requires infection of epidermal or mucosal basal cells that have the potential to proliferate and differentiate. Within these cells, overall viral gene expression is suppressed, although limited expression of specific early viral genes, including E5, E6, and E7, causes lateral expansion of infected cells within the basal layer of the epithelium (44). HPV E5 seems to be particularly important early in the course of infection. Large amounts of E5 mRNA have been found in cervical intraepithelial neoplasia (CIN) lesions (37). However, as HPV-infected lesions progress to cervical cancer, episomal viral DNA becomes integrated into host cell DNA, and a substantial part of the HPV genome, commonly including the E5 coding sequence, is deleted (16). Therefore, E5 is not obligatory in the late events of HPV-mediated carcinogenesis.

E5 is a small hydrophobic protein that can be localized within the Golgi apparatus (GA), endoplasmic reticulum

* Corresponding author. Mailing address: Department of Obstetrics and Gynecology, Faculty of Medicine, University of Tokyo, 7-3-1 Hongo, Bunkyo-ku, Tokyo 113-8655, Japan. Phone: 81-3-3815-5411. Fax: 81-3-3816-2017. E-mail: kkawana-tky@umin.ac.jp.

[▽] Published ahead of print on 1 September 2010.

(ER), and occasionally at the plasma membrane of the host cell. It has been proposed that binding of HPV16 E5 to a subunit of the cellular proton ATPase (15) is responsible for the lack of acidification of the GA and endolysosomes and the consequent impaired function of these organelles that is seen with HPV16 infection (32, 38). The presence of HPV16 E5 has also been linked to downregulation of antigen presentation by HLA class I molecules, a process that may aid in HPVs ability to evade immune clearance through cytotoxic-T-lymphocyte (CTL)-mediated adaptive immunity (1, 2, 3, 21, 30). Ashrafi and coworkers have demonstrated that HPV16 E5 retains HLA-A and -B molecules in the GA and interferes with their trafficking to the cell surface but does not alter the transcription of HLA class I heavy chains or the transporter associated with antigen processing (TAP) (2, 3, 4, 28). Others have shown that HPV16 E5 interacts with calnexin in the ER and thereby interferes with the modification of HLA class I heavy chains (21).

CD1d is an major histocompatibility complex (MHC) class I-like glycoprotein that presents self or microbial lipid antigen to natural killer T (NKT) cells (39). In humans, a specific subset of NKT cells expresses an invariant Vα24-JaQ/Vβ11 TCR (iTCR) and can recognize CD1d on the surface of antigen-presenting cells (APCs) through this receptor. CD1d is expressed not only in typical APCs (macrophages, dendritic cells, and B cells) but also in intestinal epithelial cells (8, 12), foreskin keratinocytes (9), and reproductive tract epithelial cells (25, 26). Like MHC class I, CD1d is synthesized, glycosylated by *N*-glycosyltransferase, modified, and assembled with β2m within the ER and then transferred to the GA (5, 24, 27). CD1d plays a role in both innate and adaptive immunity to various bacteria, viruses, fungi, and parasites (reviewed in reference 10). Activation of CD1d-restricted invariant NKT (iNKT) cells enhances host resistance to some microbes in a manner that depends on the level of CD1d expression on APCs (34, 35). In contrast, the activation of iNKT cells promotes susceptibility to some microbes (7, 33). The activation of CD1d-restricted iNKT cells in response to microbial invasion is antigen dependent, but these antigens can be derived from the invading microbe or possibly from host lipids (11, 22, 29). Intracellular signaling mediated by surface CD1d utilizes NF-κB, a well-known immune-related transcription factor (36, 43). CD1d-restricted NKT cells can modulate adaptive immune cells by altering Th1/Th2 polarization. Recognition of CD1d by iNKT cells can also result in rapid release of both interleukin-4 (IL-4) and gamma interferon (IFN-γ) from the NKT cell (6). Therefore, CD1d and CD1d-restricted NKT cells serve as a natural bridge between innate and adaptive immune responses to microbes. Not surprisingly, several microbes, including herpes simplex virus type 1, human immunodeficiency virus, Kaposi's sarcoma herpesvirus, and *Chlamydia trachomatis*, are known to downregulate cell surface expression of CD1d as an immune evasion strategy (13, 26, 31, 42). Our own lab previously demonstrated that *C. trachomatis* retains CD1d in the ER and targets CD1d to both chlamydial and cellular degradation pathways (26).

Viewing the importance of CD1d in innate immune responses to microbes, we hypothesized that HPV may alter CD1d-mediated immune pathways and thereby avoid innate immune destruction of the infected cell by the host. We demonstrate here that the presence of the E5 protein of HPV6 and HPV16 is associated with reduced CD1d cell surface expression. We describe a mechanism for this downregulation and hypothesize that decreased surface CD1d expression may help HPV-infected cells evade immune surveillance during the early stages of infection.

MATERIALS AND METHODS

HPV6 and HPV16 E5 expression constructs. HPV6 and HPV16 E5 open reading frames were amplified from the HPV6 and HPV16 complete genomes (kindly provided by Tadahito Kanda, National Institute of Infectious Diseases, Japan) by PCR using primers designed to introduce BamHI (forward) and EcoRI (reverse) restriction sites. The PCR products were digested with BamHI and EcoRI and subcloned into a retroviral expression plasmid pLPCX (Clontech, Mountain View, CA).

Cell lines and establishment of a cell line stably expressing CD1d. An HPV-negative human cervical carcinoma cell line, C33A, and a vaginal epithelial cell that was originally established from normal human primary epithelial cells that were immortalized by transduction with HPV16 E6/E7 genes (VK2/E6E7) (a generous gift from D. J. Anderson, Boston University, Boston, MA) (18) were grown in Dulbecco modified eagle medium (Invitrogen, Carlsbad, CA) without $CaCl_2$ (Invitrogen), supplemented with 10% fetal bovine serum (Invitrogen) at 37°C in 5% CO_2. The vaginal epithelial (VK2/E6E7) cells used here are known to express endogenous CD1d at the cell surface (25).

A CD1d-expressing retroviral plasmid pSRα-neo (kindly provided by R. Blumberg, Harvard Medical School, Boston, MA) was transfected into Phoenix cells, a packaging cell line for recombinant retroviruses (kindly provided by K. Oda, University of Tokyo), using Lipofectamine 2000 (Invitrogen). After 72 h of incubation in DMEM, the culture medium containing released CD1d-expressing retroviruses was collected and used to infect C33A cells and transfer the CD1d gene. CD1d-expressing C33A cells were selected in medium containing 1.0 mg of neomycin/ml to establish a stably transfected cell line (C33A/CD1d).

Establishment of HPV E5-expressing cell lines. HPV6 or HPV16 E5-expressing retroviral plasmids or their empty counterparts (pLPCX-16E5, pLPCX-6E5, or pLPCX, respectively) were transfected into Phoenix cells using Lipofectamine 2000 (Invitrogen). After 72 h of incubation, culture medium with released viruses were collected and used to infect C33A/CD1d or vaginal epithelial cells. Stable cell lines were selected in media containing 1.5 μg of piromycin/ml.

Immunohistochemistry. Immunostaining for CD1d was performed on formalin-fixed, paraffin-embedded tissue sections of normal or inflamed cervix, CIN1 to CIN3, cervical cancer, and condyloma acuminata (obtained under IRB approval through the University of Tokyo). A total of 45 tissues were examined. Optimal immunostaining required antigen retrieval via microwave exposure in 0.01 M citrate buffer. A mouse anti-CD1d MAb (NOR3.2, 1:100; Abcam, Inc., Cambridge, MA) or an irrelevant, isotype-matched mouse monoclonal antibody (DakoCytomation, Glostrup, Denmark) were used as primary reagents. Immunostaining was amplified and detected by using the EnVision+System-HRP (DakoCytomation). Nuclei were counterstained by using standard hematoxylin protocols (Sigma-Aldrich, Inc., St. Louis, MO). Analyses were performed at a magnification of ×200.

Flow cytometry. C33A/CD1d cells were grown in 175-cm^2 flasks until confluent, harvested using trypsin-EDTA, and pelleted at 500 × *g* for 5 min at room temperature. The cells were then washed and resuspended in PBS-B (phosphate-buffered saline [PBS] with 1% bovine serum albumin; Invitrogen) at a concentration of 10^6 cells/ml. For detection of cell surface CD1d, 100 μl of cell suspension was incubated with an anti-CD1d NOR3.2 monoclonal antibody (MAb; Abcam) at 1:100 for 30 min at 4°C. Cells were then washed three times in PBS-B, incubated with a goat anti-mouse immunoglobulin secondary antibody conjugated to phycoerythrin (PE; BD Bioscience, San Jose, CA) for 30 min at 4°C, suspended in 1% paraformaldehyde, and analyzed by using a FACSCalibur flow cytometry system (BD Bioscience).

Proteasome inhibitor treatment. C33A/CD1d cells harboring an empty vector (C33A/CD1d-empty) or expressing HPV6 E5 (C33A/CD1d-6E5) or HPV16 E5 (C33A/CD1d-16E5) were cultured for up to 24 h in the presence or absence of the cytosolic proteasome inhibitor MG132 (10 μM in dimethyl sulfoxide [DMSO]; Sigma-Aldrich, Inc.). Control wells included vehicle alone.

HPV genotyping. DNA was extracted from cervical smear samples by using the DNeasy blood minikit (Qiagen, United Kingdom). HPV genotyping was performed by using the PGMY-CHUV assay method (20). Briefly, standard PCR was conducted using the PGMY09/11 L1 consensus primer set and HLA-dQ primer sets (20). Reverse blotting hybridization was performed as described

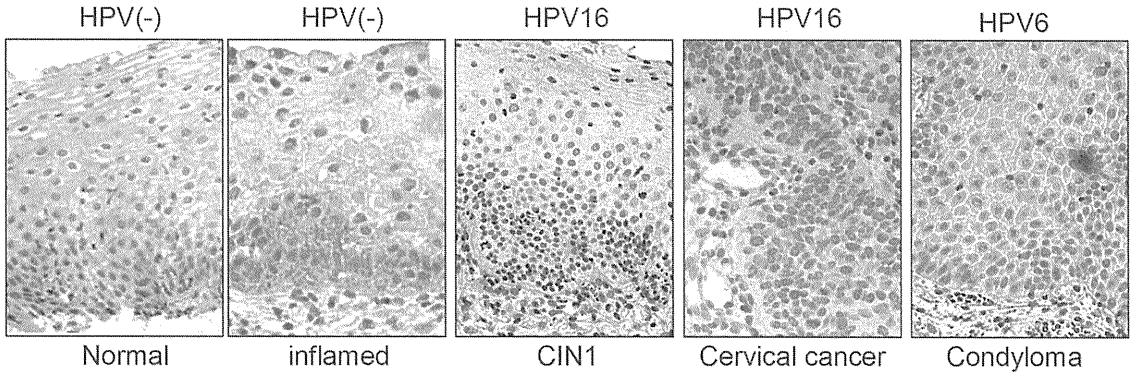

FIG. 1. Immunostaining of HPV-associated lesions for CD1d. Immunostaining for CD1d was performed after antigen retrieval on formalin-fixed, paraffin-embedded tissue sections of HPV-negative normal and inflamed ectocervical epithelium, HPV16-positive CIN1, HPV16-positive cervical cancer, and HPV6-positive condyloma acuminata. CD1d was detected with NOR3.2, a CD1d-specific MAb (1:100).

previously (20). Heat-denatured PCR amplicons were hybridized to a negatively charged nylon membrane containing specific probes for 32 HPV genotypes and HLA-dQ reference samples. Chemiluminescence detection used enhanced chemiluminescence (ECL) detection reagents for nucleic acids (GE Healthcare). Films were interpreted using the HPV reference guide provided.

RT-PCR and quantitative PCR. Portions (1 μg) of total RNA and oligo(dT)s were used for reverse transcriptase (RT) reactions (RNA PCR kit; Applied Biosystems, Foster City, CA). Total cDNA reaction samples were used as templates for amplification of each gene fragment using a PCR Core kit (Applied Biosystems). Primer pair sets for CD1d were synthesized by Invitrogen (CD1d, 453 bp; 5′-GCTGCAACCAGGACAAGTGGACGAG-3′ [forward] and 5′-AG GAACAGCAAGCACGCCAGGACT-3′ [reverse]). Those for IL-12 p40 were commercially available (Sigma-Aldrich, Inc.). For quantitative PCR, cDNA were produced via RT of 1 μg of total RNA extracted from the cells as described above by using an OmniScript RT kit (Qiagen, Inc., Valencia, CA). Portions (2 μl) of 5-fold-diluted cDNA aliquots were amplified in a thermal cycler (7300 Real-Time PCR System; Applied Biosystems) by using a QuantiTect SYBR green PCR kit (Qiagen, Inc.) and a primer pair set for β-actin (5′-GAAATCG TGCGTGACATTAAGG-3′[forward] and 5′-TCAGGCAGCTCGTAGCTTC T-3′ [reverse]). The mRNA levels for IL-12 were normalized to those of β-actin, the internal control.

Fluorescent deconvolution microscopy and confocal microscopy. C33A/CD1d cells were seeded onto coverslips. The ER was visualized using the ER tracker Blue-White DPX (Invitrogen) for 30 min at 37°C. All coverslips were fixed in 4% paraformaldehyde, permeabilized with 0.1% Tween 20. They were then incubated for 1 h at 37°C with either an anti-CD1d NOR3.2 MAb labeled with Zenon Alexa Fluor 555 using a mouse IgG labeling kit (Invitrogen) or an anti-FLAG MAb labeled with Zenon Alexa Fluor 488 using a mouse IgG labeling kit (Invitrogen) singly or in combination. With the exception of ER tracker-treated coverslips, the cells were then counterstained with a DAPI (4′,6′-diamidino-2-phenylindole) nucleic acid stain (Invitrogen). Images were obtained with a LSM 700, flexible confocal microscope (Carl Zeiss, Oberkochen, Germany). Filter sets were optimized for Alexa 488, Alexa 555, and DAPI. Z-axis plane capture, deconvolution, and analyses were performed with ZEN 2009 Software (Carl Zeiss).

Western blotting. Portions (50 μg) of total cell lysates from C33A/CD1d-empty, C33A/CD1d-6E5, or C33A/CD1d-16E5 cells in a modified TNF buffer (1 M Tris-HCl [pH 7.8], 10% NP-40, 5 M NaCl, 0.5 M EDTA [pH 8.0], aprotinin, 0.1 M phenylmethylsulfonyl fluoride) were electrophoresed and transferred to nitrocellulose membranes. Membranes were blocked with 10% milk and incubated with a peroxidase-labeled anti-CD1d NOR3.2 MAb (1:200; Abcam) or an anti-FLAG MAb (1:500; Sigma-Aldrich, Inc.) using a peroxidase labeling kit (Roche, Basel, Switzerland) for 1 h. Membranes were washed and bound antibody was detected using an ECL Western blotting analysis system (GE Healthcare Buckinghamshire, United Kingdom).

Immunoprecipitation and Western immunoblotting. Harvested C33A/CD1d-empty, C33A/CD1d-6E5, or C33A/CD1d-16E5 cells were lysed in modified radioimmunoprecipitation assay buffer (1% NP-40, 1% deoxycholate, 0.1% sodium dodecyl sulfate [SDS], 10 mM Tris, 150 mM NaCl, 2 mM EDTA) with protease inhibitors (Amersham Biosciences, Piscataway, NJ). Equivalent aliquots of total cell lysates were incubated overnight at 4C with 5 μg of mouse anti-FLAG MAbs (Sigma-Aldrich, Inc.)/ml and 5 μl of protein A-Sepharose (GE Healthcare). Precipitated proteins were separated by SDS-PAGE using 7.5% acrylamide gels and transferred to polyvinylidene difluoride membranes. Mouse anti-calnexin or rabbit anti-β-actin polyclonal antibodies (Abcam) were used as primary reagents for immunoblotting, and anti-mouse IgG-HRP (1:100,000; GE Healthcare) was used as a secondary reagent. Products in Western immunoblotting experiments were visualized by using an ECL Western blotting analysis system (GE Healthcare). Molecular masses were confirmed by comparison to standard size markers (GE Healthcare).

Statistical analysis. Quantitative PCR data were presented as means ± the standard deviations. Experiments were performed independently at least three times. The Cochran-Armitage Trend test was computed to show trends in immune reactivity with NOR3.2 MAb in clinical samples. IL-12 mRNA levels were compared to those before or after cross-linking by using paired, two-tailed Student *t* tests. A P value of <0.05 was considered significant.

RESULTS

CD1d downregulation in HPV-related lesions and cancer cell lines. Since CD1d expression in human mucosa and skin has been demonstrated by immunohistochemistry using the anti-CD1d NOR3.2 MAb (2, 9, 12, 26), we examined immunostaining of human normal ectocervix or HPV-related lesions with NOR3.2 (Fig. 1). Immunostaining for CD1d was performed on formalin-fixed, paraffin-embedded tissue sections of normal or inflamed ectocervical epithelium, cervical intraepithelial neoplasia 1 (CIN1), cervical cancer, and cervical condyloma (obtained under IRB approval through the University of Tokyo, Faculty of Medicine). To examine alterations in CD1d expression in the presence of high-risk HPV and low-risk HPV subtypes, HPV16-positive CIN1 or cancer lesions and HPV6-positive condyloma acuminata specimens were compared to each other and to HPV-negative normal and inflamed ectocervical epithelial controls. Immunoreactivity with the NOR3.2 MAb was noted in the basal and parabasal epithelial cells of normal and inflamed ectocervical epithelia that are known to express early HPV genes (E5, E6, and E7; Fig. 1) (44). In inflamed epithelium, the immunoreactivity appeared to be intensified compared to normal epithelium. CD1d expression is known to be enhanced by inflammatory cytokines (10). NOR3.2 immunoreactivity is essentially absent in HPV16-positive CIN1, HPV16-positive cancer, and HPV6-positive condyloma lesions (Fig. 1). To statistically analyze alterations in CD1d expression, a total of 45 clinical specimens from normal controls and HPV-related lesions were immunostained with NOR3.2 (Table 1). NOR3.2 immunoreactivity was

TABLE 1. Immunoreactivity with NOR3.2 anti-CD1d MAb in cervical epithelium of various lesions

Histological status	HPV status[a]	CD1d (no. of cases)		% Positive[b]
		Positive	Negative	
Normal/inflamed		9	1	90.0
CIN1 and CIN2	HR-HPV(+)	0	7	0
CIN3	HR-HPV(+)	2	16	11.1
Cancer	HR-HPV(+)	0	7	0
Condyloma	HPV6(+)	0	3	0

[a] HR-HPV(+), any high-risk HPV positive.
[b] $P = 0.0001$ (exact Cochran-Armitage Trend test).

mostly limited to the HPV-negative normal or inflamed ectocervical epithelial samples similar to those represented in the first two panels of Fig. 1. NOR3.2 immunoreactivity was absent in all CIN1 and CIN2, cervical cancer, and condyloma lesions. Among CIN3 samples, two lesions showed NOR3.2 immunoreactivity, whereas 16 lesions did not. Using trend analysis, we were able to demonstrate an association between decreased CD1d immunoreactivity and progression of cervical neoplastic lesions with statistical significance ($P = 0.0001$).

Although HPV E5 is not expressed in cervical cancer cells (16), immunohistochemical data demonstrated that CD1d expression was also abrogated in cervical cancer lesions. To address the mechanisms underlying CD1d downregulation in cervical cancers, we examined the level of CD1d transcription and CD1d expression at the cell surface in several cervical cancer cell lines (Fig. 2). As a positive control, we created cell transfectants that stably expressed CD1d. To avoid the potential influence of endogenous HPV protein expression, an HPV-negative cervical cancer cell line, C33A, was used for our CD1d transfectants. We used a retrovirus vector to transduce the CD1d gene into these cells and established the stable cell line, C33A/CD1d via neomycin selection. Flow cytometry revealed strong expression of CD1d on the cell surface of C33A/CD1d cells. Cd1d was not expressed on the cell surface of C33A control cells or in other cancer cell lines (Fig. 2A). To examine the level of CD1d transcription in these same cells, cDNA was produced via RT of total RNA from each cell line and subjected to PCR using primer pairs specific for CD1d. The expected single band representing CD1d was observed on agarose gels only in C33A/CD1d cells (Fig. 2B). These data indicated that CD1d expression was abrogated prior to or during transcription the tested cervical cancer cell lines.

Cell surface expression of CD1d decreases in HPV E5-expressing epithelial cells. HPV E5 has been reported to inhibit cell surface expression of HLA class I molecules by interfering with their trafficking to the cell surface (1, 2, 3, 21, 30). Since CD1d and HLA class I heavy chains utilize an identical intracellular pathway to traffic from the ER to the cell surface, we hypothesized that HPV E5 may also interfere with surface CD1d expression at a posttranscriptional level. To verify our immunohistochemical data and study CD1d trafficking in the presence of E5 *in vitro*, we created HPV6 and HPV16 E5 stably transfected cell lines using C33A/CD1d cells. Since the E5 protein is less than 10 kDa in size, the production of an anti-E5 antibody would be difficult. Instead, E5 proteins were tagged with FLAG and detected by Western blotting or immunostaining with an anti-FLAG antibody. FLAG-tagged HPV6 or HPV16 E5 genes were transduced into the C33A/CD1d cells by using retrovirus vectors. To control for the influence of retrovirus infection and the presence of the expression vector, C33A/CD1d cells were infected with empty retrovirus vectors. Retrovirus-infected cells were exposed to puromycin, and E5-expressing C33A/CD1d cells were established (C33A/CD1d-6E5, -16E5, and -empty). In Fig. 3A, lanes 5 and 6, show PCR products derived from cDNA generated by RT of total RNA from C33A/CD1d-6E5 and -16E5 cells. Lanes 2 and 3 in the same figure show PCR products derived from corresponding expression plasmid DNA. FLAG-6E5 and -16E5 were transcribed in C33A/CD1d-6E5 and -16E5 cells, respectively. Using Western immunoblotting and an anti-FLAG MAb, FLAG-6E5 and -16E5 proteins were detected as immunoreactive bands at an approximate size of 10 kDa in lanes 1 and 2, respectively (Fig. 3B).

We next examined the expression of CD1d at both mRNA and protein levels in the presence or absence of HPV E5. CD1d transcription levels in C33A/CD1d cells were unaffected by the presence of E5 or of empty vector compared to naive

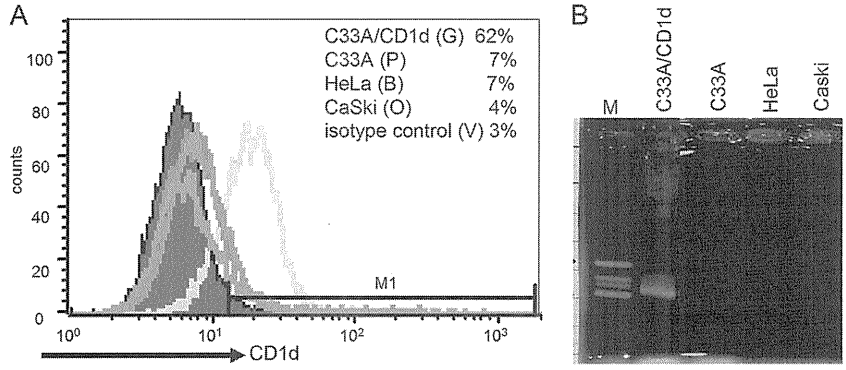

FIG. 2. CD1d alterations in cancer cell lines. (A) Cell surface expression of CD1d in C33A (pink line), HeLa (blue line), CaSki (orange line), and C33A/CD1d (green line) cells. All cells were stained with an anti-CD1d primary MAb (NOR3.2; 1:100 dilution) and a PE-conjugated goat anti-mouse immunoglobulin secondary antibody (1:20 dilution). Background staining of the cells using an isotype-matched control antibody is also shown (filled region). Cells were suspended in 1% paraformaldehyde and analyzed by using a FACSCalibur flow cytometry system. (B) Transcription of CD1d. cDNA was produced via RT of 1 μg of total RNA from each cell line and amplified by PCR with primer pairs specific for CD1d. PCR products were separated over an agarose gel containing ethidium bromide.

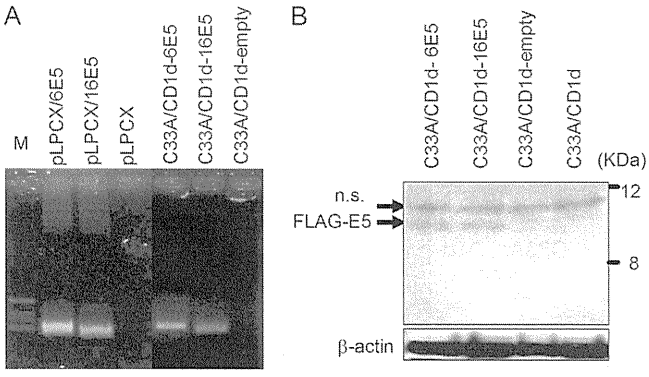

FIG. 3. HPV E5 detection in HPV E5-transformed C33A/CD1d cells. (A) Transcription of HPV E5. cDNA was produced via RT of 1 μg of total RNA from each cell line and amplified by PCR with primer pairs specific for HPV16 E5 and HPV6 E5. PCR products were separated over an agarose gel containing ethidium bromide. Lanes 5 and 6 display PCR products derived from C33A/CD1d-6E5 and -16E5 cDNA, respectively, while lanes 2 and 3 show PCR products derived from corresponding expression plasmid DNA. Lanes 4 and 7 represent negative control plasmid and cell lines lacking E5, respectively. (B) Translation of HPV E5. Fifty-microgram aliquots of protein lysates from each cell line were analyzed by Western immunoblotting with antibodies against the FLAG tag (1:500 dilution) and β-actin (loading control).

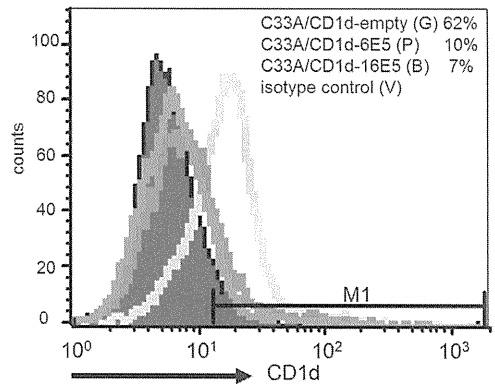

FIG. 5. Cell surface expression of CD1d in C33A/CD1d-empty (green line), C33A/CD1d-6E5 (pink line), and -16E5 (blue line) cells. All cells were stained with an anti-CD1d primary MAb (NOR3.2; 1:100 dilution) and a PE-conjugated goat anti-mouse immunoglobulin secondary antibody (1:20 dilution). Background staining of the cells with an isotype-matched control antibody is also shown (filled region). Cells were suspended in 1% paraformaldehyde and analyzed using a FACSCalibur flow cytometry system.

C33A/CD1d cells (Fig. 4A). In contrast, the 48-kDa, mature glycosylated form of the CD1d heavy chain (HC) that was detected in naive C33A/CD1d and C33A/CD1d-empty cells was completely abrogated in C33A/CD1d-6E5 and barely detectable in the C33A/CD1d-16E5 cells (Fig. 4B, lanes 1, 4, 2, and 3, respectively). The presence of HPV6 and HPV16 E5 drastically inhibited the maturation of CD1d HCs. Flow cytometry was used to analyze the effect of HPV E5 on cell surface expression of CD1d in the C33A/CD1d cells harboring E5-expressing or empty vector (Fig. 5). CD1d was expressed by

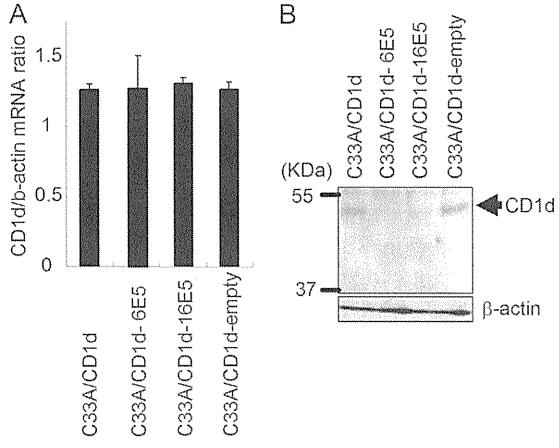

FIG. 4. CD1d heavy-chain transcription and translation in C33A/CD1d, C33A/CD1d-empty, C33A/CD1d-6E5, and C33A/CD1d-16E5 cells. (A) Transcription of CD1d HC. The mRNA levels of CD1d were analyzed by quantitative RT-PCR using SYBR green methodology. CD1d mRNA levels were normalized to β-actin. (B) Fifty-microgram aliquots of protein lysates from each cell line were analyzed by Western immunoblotting with a peroxidase-labeled anti-CD1d NOR3.2 MAb (1:200 dilution) and a β-actin loading control.

the majority of C33A/CD1d-empty cells but absent in >70% of C33A/CD1d-6E5 or -16E5 cells (Fig. 5).

To confirm the effect of E5 on endogenous CD1d, we used a vaginal epithelial cell line immortalized via HPV16 E6/E7 transduction of primary cells collected from normal human vaginal epithelium and subsequently well characterized as possessing histological and immunological characteristics identical to those of primary epithelial cells (18). We have previously reported the endogenous expression of functional CD1d molecules on the surface of these cells (25). Since vaginal epithelial cells are well-known targets of genital HPV, these cells were considered to be useful as an *in vitro* model for *in vivo* HPV infections. FLAG-tagged HPV6 or HPV16 E5 genes were transduced into these vaginal cells by using retrovirus vectors (Vag-6E5 and -16E5). We then examined the expression of CD1d at various levels in the presence or absence of HPV E5 (Fig. 6). RT-PCR and Western blotting revealed that CD1d transcription was unaffected by the presence of E5, but the 48-kDa CD1d HC product clearly decreased in Vag-6E5 and -16E5 cells compared to naive and Vag-empty cells (Fig. 6A). Flow cytometry confirmed the decreased cell surface expression of CD1d in 6E5-expressing vaginal epithelial cells (Fig. 6B).

E5-expressing epithelial cells retain CD1d in the ER. To demonstrate the intracellular localization of CD1d heavy chains in C33A/CD1d cells harboring HPV-6E5 and -16E5, immunofluorescence confocal microscopy was performed with an anti-CD1d MAb (NOR3.2) combined with either an anti-FLAG MAb that detects FLAG-E5 proteins, an ER-specific marker (ER tracker) or DAPI (Fig. 7). In C33A/CD1d-empty control cells, dual labeling for CD1d and the nucleus (DAPI) verified that CD1d could be detected in a diffuse pattern throughout the intracellular space, with increased accumulation near the cell surface but not in the perinuclear area (Fig. 7, upper image). In contrast, decreased amounts of CD1d could be detected in C33A/CD1d-6E5 and -16E5 cells and CD1d proteins were localized to perinuclear areas near the ER. CD1d and ER signals merged in perinuclear areas (pink

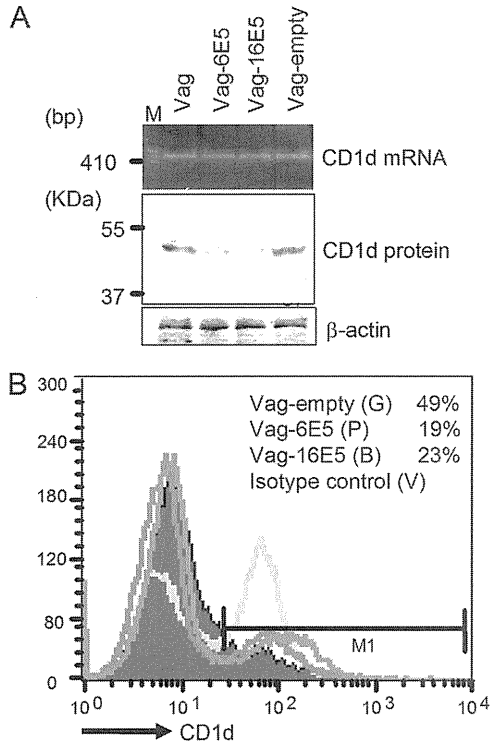

FIG. 6. CD1d downregulation in alternate genital keratinocytes in the presence of 6E5 and 16E5. (A) HPV6 and HPV16 E5 genes were transduced into vaginal epithelial cells established from normal human vaginal epithelium (17) and named Vag-6E5 and Vag-16E5, respectively. PCR products derived from cDNA generated by reverse transcription using 1 μg of total RNA from each of the vaginal cell lines were separated over an ethidium bromide-containing agarose gel. Fifty-microgram aliquots of protein lysates from each vaginal cell line were analyzed by Western immunoblotting with a peroxidase labeled anti-CD1d NOR3.2 MAb (1:200 dilution) and a β-actin loading control. (B) Vag-empty (green line), Vag-6E5 (pink line), and Vag-16E5 (blue line) were stained with an anti-CD1d primary MAb (NOR3.2; 1:100 dilution) and a PE-conjugated goat anti-mouse immunoglobulin secondary antibody (1:20 dilution). Background staining of the cells using an isotype-matched control antibody is also shown (filled region). Cells were suspended in 1% paraformaldehyde and analyzed by using a FACSCalibur flow cytometry system.

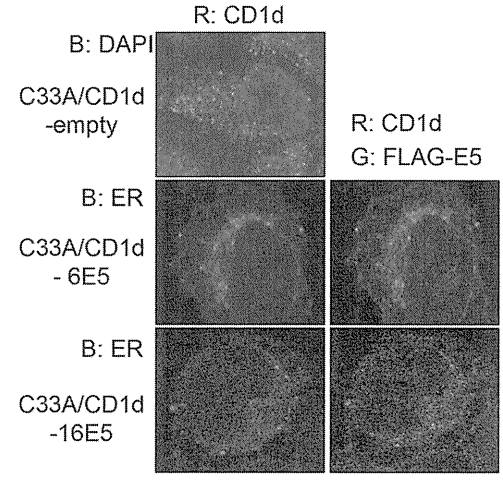

FIG. 7. CD1d trafficking in the presence or absence of E5. C33A/CD1d-empty, C33A/CD1d-6E5, or C33A/CD1d-16E5 cells were seeded onto coverslips. All of the cells were immunostained with an anti-CD1d MAb (NOR3.2, red). C33A/CD1d-empty were also exposed to DAPI (blue), and C33A/CD1d-6E5 or -16E5 cells were exposed to ER tracker (blue) and an anti-FLAG MAb (green). Cells were then visualized by using fluorescence confocal microscopy. Orange to yellow signals represent colocalization of CD1d and E5 within the ER.

signals), suggesting that the majority of CD1d is within the ER (Fig. 7, images on the left). Dual labeling for CD1d and FLAG-E5 verified the colocalization of CD1d and E5 within the ER (orange to yellow signals), while nonmerged FLAG-E5 signals were present in the perinuclear area (pure green), suggesting the presence of E5 in the GA in the absence of CD1d (Fig. 7, images on the right). The results of immunofluorescence microscopy support our biochemical and flow cytometry data showing that mature CD1d protein levels decrease and CD1d fails to traffic to the cell surface in HPV E5-expressing cells.

HPV E5 interacts with calnexin in the ER. Previous biochemical studies have reported that HPV16 E5 interacts with calnexin and that these interactions interfere with the modification of HLA class I heavy chains that typically occurs in the ER (21). The role of calnexin and/or calreticulin in the formation of the second disulfide bond of CD1d HCs in the ER is well described (24). We therefore hypothesized that E5 interacts with calnexin in the ER and may impair calnexin-mediated CD1d folding. This, in turn, could interrupt appropriate trafficking of CD1d to the surface of HPV-infected cells. To address the hypothesis, we examined the interaction of E5 with calnexin using immunoprecipitation. Total cell lysates obtained from C33A/CD1d-empty, -6E5, and -16 E5 cells were incubated with anti-FLAG MAb conjugated beads. FLAG-E5-bound proteins were immunoprecipitated and analyzed by immunoblotting with an anti-calnexin MAb. A band with an apparent molecular mass of 90 kDa and corresponding to calnexin was detected in C33A/CD1d-6E5 and -16 E5 cells, but not C33A/CD1d-empty cells, biochemically demonstrating interaction between E5 with calnexin (Fig. 8A).

To visually demonstrate the colocalization of CD1d and calnexin, C33A/CD1d-empty, -6E5, and -16E5 cells were dually stained with anti-CD1d NOR3.2 and anti-calnexin MAbs and examined by using confocal microscopy. Again, NOR3.2-reactive CD1d was detected throughout the intracellular space in C33A/CD1d-empty cells. In contrast, the majority of CD1d molecules in C33A/CD1d-6E5 or -16E5 cells localized to the perinuclear area (Fig. 8B, images on left). Calnexin detection was rendered as green signals. These mostly localized to perinuclear areas in E5-expressing cells and correspond to the location of ER (Fig. 8B, center images). Although some merge images (yellow signals) could be detected in each cell line, the merge patterns differed between C33A/CD1d-empty and E5-expressing cells (Fig. 8B, images on the right). In C33A/CD1d-empty cells, the calnexin and CD1d signals were mostly distinct and but those that did colocalize appeared to follow the synthetic pathway for type I proteins. In contrast, CD1d in the E5-expressing cells completely colocalized with calnexin, confirming our biochemical data demonstrating physiologic interaction between calnexin and CD1d in the C33A/CD1d-6E5 and -16E5 cells.

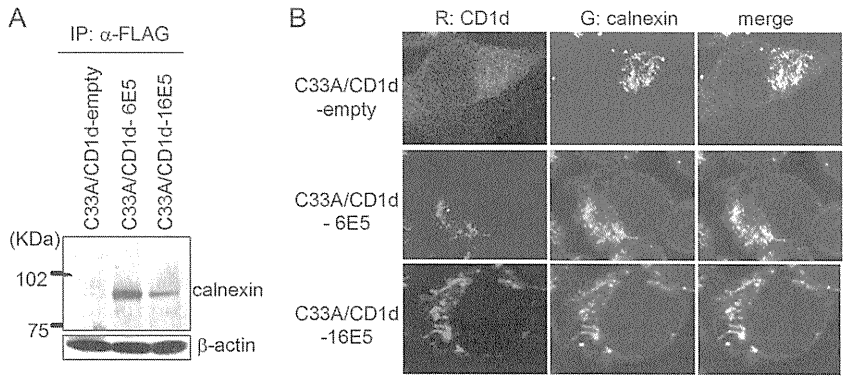

FIG. 8. CD1d and calnexin have direct interactions and colocalize in the perinuclear area in the presence of HPV E5. (A) Protein lysates from C33A/CD1d-empty, C33A/CD1d-6E5, and C33A/CD1d-16E5 cells were immunoprecipitated with an anti-FLAG MAb. Immunoprecipitants were then separated by SDS-PAGE and immunoblotted with an anti-calnexin antibody. (B) C33A/CD1d-empty, C33A/CD1d-6E5, or C33A/CD1d-16E5 cells were seeded onto coverslips. All cells were exposed to an anti-CD1d MAb (NOR3.2, red) and to an anti-calnexin MAb (green) labeled with Zenon Alexa Fluor 488 using a mouse IgG labeling kit. Cells were then visualized by using fluorescence confocal microscopy. Yellow images represent colocalization of CD1d and calnexin.

CD1d was rescued by treatment of proteasome inhibitor. We have previously demonstrated that surface expression of CD1d in human genital epithelial cells is downregulated by *C. trachomatis* infection and that downregulation involves chlamydial protein-mediated proteasomal pathways (26). We hypothesized that HPV infection could utilize posttranslational cellular proteasomal degradation to inhibit cell surface expression of CD1d HC. To address the role of the cellular proteasome in E5-associated CD1d degradation, C33A/CD1d-empty, -6E5, or -16E5 cells were exposed to the proteasome inhibitor, MG132, and CD1d HC levels in cell lysates compared to those in unexposed cells (Fig. 9). Using the NOR3.2 MAb for immunoblotting, the reduced or abrogated expression of the 48-kDa mature CD1d HC in E5-expressing cells could be rescued by the presence of MG132 (Fig. 9A). To visually replicate this effect, immunofluorescence microscopy was performed with the NOR3.2 MAb and DAPI in MG132 exposed and unexposed E5-expressing and control cells (Fig. 9B). In C33A/CD1d-empty cells, NOR3.2-reactive CD1d was detected throughout the intracellular space (Fig. 9B, upper left image). In contrast, NOR3.2-reactive CD1d was barely detected or undetectable in the majority of unexposed C33A/CD1d-6E5 or -16E5 cells (Fig. 9B, upper, right two images). In the presence of proteasomal inhibition with MG132, E5-expressing cells again show CD1d signals throughout the intracellular space (Fig. 9B, lower panels). HPV E5-expressing cells completely recover their expression mature CD1d molecules upon inhibition of cellular proteasomal degradation.

HPV E5 abrogates CD1d-mediated cytokine production in the epithelial cells. Surface CD1d interacts specifically with iNKT cells bearing an iTCR. The interaction not only activates NKT cells but also induces phosphorylation of CD1d, intracellular signaling, and the release of cytokines from the CD1d-bearing cell. We have previously demonstrated that human reproductive tract epithelial cells expressing CD1d on their cell surfaces have the capacity to produce cytokines, especially IL-12, after CD1d ligation (25). IL-12 is a central mediator in both innate and adaptive immunity and is crucial in the prevention of many infectious diseases and tumors (40). IL-12 induces IFN-γ-producing NK, NKT, T helper, and cytotoxic T cells. Since our investigations had demonstrated a decrease in cell surface expression of CD1d in the presence of HPV and specifically of HPV E5, we next examined whether CD1d-mediated IL-12 production was abrogated in E5-expressing epithelial cells (Fig. 10). An anti-CD1d 51.1 MAb can be used for CD1d cross-linking and represents an *in vitro* model for

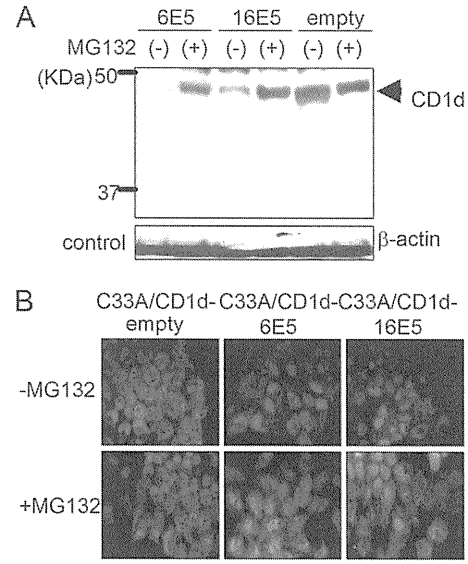

FIG. 9. Proteasome inhibition rescues CD1d from E5-mediated degradation. (A) C33A/CD1d-empty, C33A/CD1d-6E5, or C33A/CD1d-16E5 cells were cultured for up to 24 h in the presence or absence of the cytosolic proteasome inhibitors MG132 (10 μM) in DMSO. Fifty micrograms of protein lysates from each cell line were analyzed by Western immunoblotting with a peroxidase-labeled anti-CD1d MAb (NOR3.2; 1:200 dilution) and a β-actin loading control. (B) C33A/CD1d-empty, C33A/CD1d-6E5, or C33A/CD1d-16E5 cells were seeded onto coverslips and cultured for up to 24 h in the presence (lower) or absence (upper) of MG132 (10 μM) in DMSO. All coverslips were fixed in 4% paraformaldehyde, permeabilized with 0.2% Triton-X, blocked with 6% BSA, and incubated for 1 h at room temperature with an anti-CD1d NOR3.2 MAb (red) directly conjugated with Zenon Alexa Fluor 555 using a mouse IgG1 labeling kit. Cells were then counterstained with a DAPI (blue) nucleic acid stain.